AD NUMBER

AD270535

NEW LIMITATION CHANGE

TO

Approved for public release, distribution unlimited

FROM

Distribution authorized to U.S. Gov't. agencies and their contractors; Administrative/Operational Use; Nov 1961. Other requests shall be referred to Aeronautical Systems Div., Wright-Patterson AFB, OH 45433.

AUTHORITY

AFFDL ltr, 21 oct 1974

UNCLASSIFIED

AD 270 535

Reproduced
by the

ARMED SERVICES TECHNICAL INFORMATION AGENCY
ARLINGTON HALL STATION
ARLINGTON 12, VIRGINIA

UNCLASSIFIED

ASD TECHNICAL REPORT 61-326

DETERMINATION OF THE MINIMUM SIZED PARACHUTE REQUIRED FOR STABILIZATION OF THE A-22 CARGO CONTAINER

HELMUT G. HEINRICH
AND
SHUKRY K. IBRAHIM

DEPARTMENT OF AERONAUTICAL ENGINEERING
UNIVERSITY OF MINNESOTA

NOVEMBER 1961

AERONAUTICAL SYSTEMS DIVISION

ASD TECHNICAL REPORT 61-326

DETERMINATION OF THE MINIMUM SIZED PARACHUTE REQUIRED FOR STABILIZATION OF THE A-22 CARGO CONTAINER

HELMUT G. HEINRICH
AND
SHUKRY K. IBRAHIM

DEPARTMENT OF AERONAUTICAL ENGINEERING
UNIVERSITY OF MINNESOTA

NOVEMBER 1961

AERODYNAMIC DECELERATOR BRANCH
FLIGHT ACCESSORIES LABORATORY
CONTRACT No. AF 33(616)-6372
PROJECT 6065
TASK 60252

AERONAUTICAL SYSTEMS DIVISION
AIR FORCE SYSTEMS COMMAND
UNITED STATES AIR FORCE
WRIGHT-PATTERSON AIR FORCE BASE, OHIO

200 - January 1962 - 19-777

FOREWORD

This report was prepared by the Department of Aeronautical Engineering of the University of Minnesota in compliance with US Air Force Contract No AF 33(616)-6372.

The work being accomplished under this contract is sponsored jointly by QM Research and Engineering Command, Department of the Army; Bureau of Naval Weapons, Department of the Navy; and Air Research and Development Command (now designated Air Force Systems Command), Department of the Air Force, and is directed by a Tri-Service Steering Committee concerned with Aerodynamic Retardation. Contract administration is conducted by Aeronautical Systems Division and Mr. Rudi J. Berndt of the Aerodynamic Decelerator Branch, Flight Accessories Laboratory, Wright Air Development Division, is Project Engineer.

Messrs. Edward Holmbeck and Bruce Gniffke and a number of graduate and undergraduate students contributed significantly to this study, and the authors wish to express their appreciation to them.

ABSTRACT

An investigation to determine experimentally the minimum size and optimum type of parachute for stabilizing general aerial delivery cargo and more specifically, the A-22 Cargo Container, was conducted. It was found that a 4 ft ribless guide surface parachute in connection with a riser at least 10 ft long represented the desired optimum. A 64 in. ribbon parachute with 20% geometric porosity in connection with a minimum riser length of 10 ft appeared also to be quite satisfactory.

In addition, the investigation provided sufficient data for the calculation of trajectories for different configurations and release conditions.

PUBLICATION REVIEW

This report has been reviewed and is approved.

FOR THE COMMANDER:

George A. Solt, Jr.
Chief, Retardation and Recovery Branch
Flight Accessories Laboratory

TABLE OF CONTENTS

LIST OF ILLUSTRATIONS

LIST OF SYMBOLS

C_D	Drag coefficient, general
C_{D_c}	Container drag coefficient (referred to container base area)
C_{D_p}	Parachute drag coefficient (referred to container base area)
C_{D_o}	Drag coefficient of parachute canopy based on total cloth area, S_o
C_{D_s}	System drag coefficient (referred to container base area)
C_M	Moment coefficient (referred to container base area and length of base diagonal)
D	Drag, general (lb)
D_o	Nominal canopy diameter
D_p	Projected or inflated canopy diameter
H	Container height dimension
L	Lift, general (lb)
q	Dynamic pressure assuming incompressible fluid (lb per sq ft)
Re	Reynolds number
S_o	Total cloth area of a canopy
S_p	Projected area of inflated canopy
W	Weight, general
α	Container angle of attack (degrees)
θ	Angle of yaw of parachute with respect to the container's longitudinal axis (degrees)
ψ	Angle of pitch of parachute with respect to the container's longitudinal axis (degrees).

I. INTRODUCTION

The basic objective of this project is to determine the minimum size and optimum parachute type capable of stabilizing general aerial delivery cargo and more specifically the United States Army A-22 Cargo Container.

1.1 A-22 Container and Standard Aerial Delivery System

A description of the A-22 Container with illustrations is given in the Department of the Army Technical Manual TM-530 of June, 1952, (Ref 1). This manual was provided by the Procuring Agency together with drawings of the component parts of the container, namely the sling, inner liner, skid, and web. Appendix IIIc, p 46 of Ref 1 lists the suggested loads and main dimensions of typical cargo for the A-22 Container. The maximum dimensions for the base are 52 in. x 43 in. and the height varies between 60 in. (max) and 40 in. (min). The A-22 Container was designed for delivery by the floor level roller conveyor system using the G-12D parachute. This is a 64 ft diameter, flat circular parachute with the following characteristics (Ref 2, p 2-1-3):

Rated Weight Capacity	2,200 lbs
C_{D_o}	0.75
Angle of Oscillation	30° (approx)
Air Drop Speed Limit	175 knots
Rate of Descent (with 2,200 lbs load)	27.6 ft/sec
Weight	126 lbs

Manuscript released by the authors on July, 1961, for publication as an ASD Technical Report.

1.2 High Velocity Aerial Delivery

Recent trends in the aerial delivery of cargo require much higher rates of descent, of the order of 75 ft per second or more, together with more stringent stability requirements and the use of energy dissipating, cushioning devices at ground impact. Reference 3 shows that by using a 22 ft ringslot parachute giving a rate of descent of about 75 ft per second, together with paperboard honeycomb as cushioning material, the following advantages could be achieved:

1) Greater drop accuracy
2) Reduced dispersion due to wind effects
3) Considerable reduction in the cost of aerial delivery.

To assure a high degree of efficiency of this system, the longitudinal axis of the parachute load system shall not deviate more than five degrees from the tangent of the ballistic trajectory. The main objective of this study is to determine the type and size of a parachute which would fulfill this requirement with a minimum amount of parachute drag.

II. EXPERIMENTAL EQUIPMENT

2.1 Wind Tunnel

The experimental tests were conducted in the open test section arranged in the return circuit of the University of Minnesota subsonic wind tunnel. Figure 1 is a schematic layout of this tunnel giving its main dimensions and indicating the modifications introduced in the return circuit of the wind

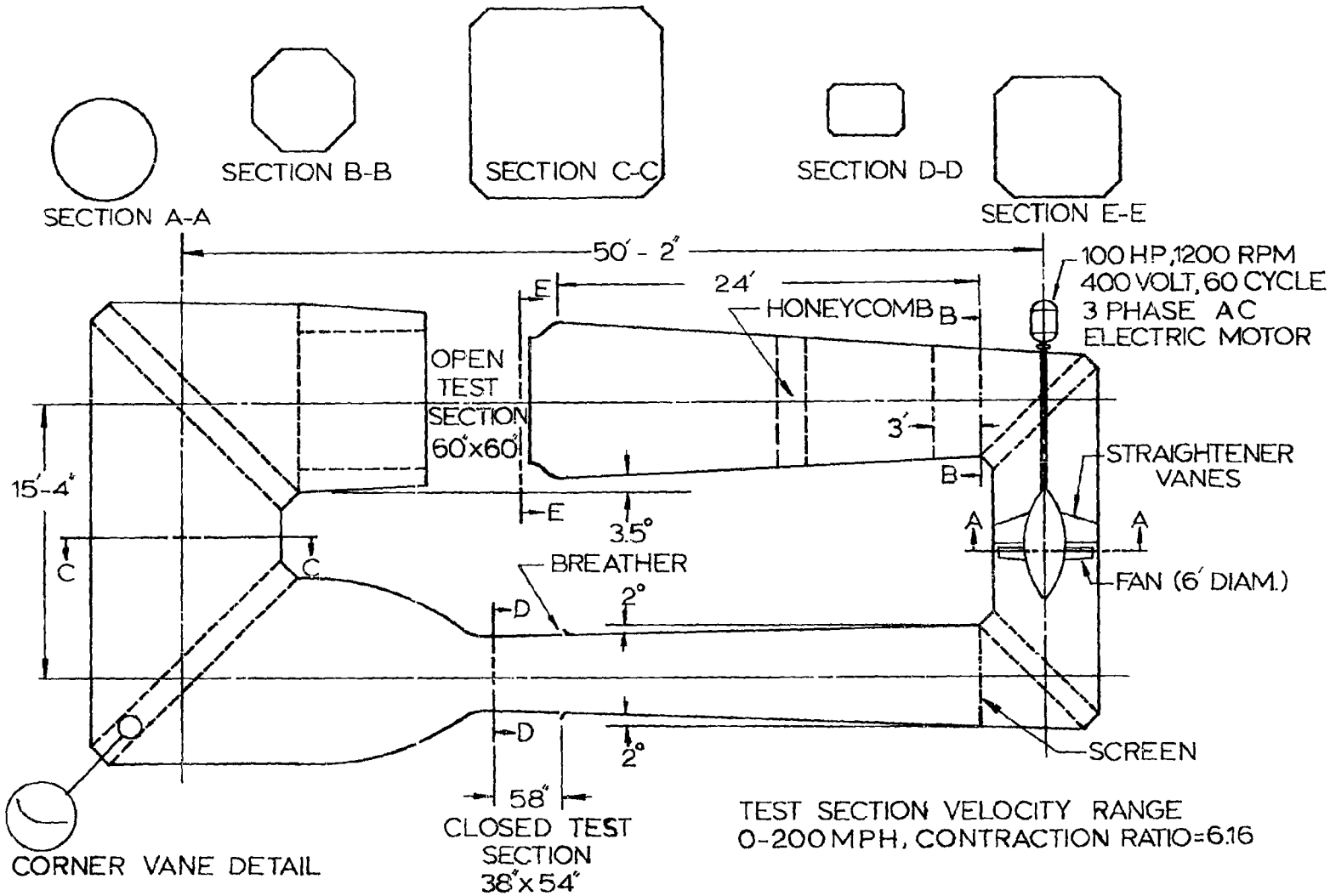

FIG. 1- UNIVERSITY OF MINNESOTA HORIZONTAL RETURN WIND TUNNEL, SCHEMATIC LAYOUT

tunnel to provide an open test section (Free Jet). Figure 2 is a photograph showing the honeycomb and contraction sections upstream of the open test section.

2.2 Model Mounting Frame

A special frame for mounting the A-22 Container and parachute models was built and is illustrated in Fig 3. When mounted in this frame, the A-22 Container model is free to rotate about an axis perpendicular to the air stream. The design of the frame is such that the pivotal axis may be set vertically (as shown in Fig 3A) or horizontally (Fig 3B). In the vertical mounting position, gravity effects on the container may be neglected and only the aerodynamic forces and moments will be effective. The vertical mounting position was used in all tests reported here and Fig 4 illustrates with main dimensions the general layout of the model and mounting frame in the open test section.

The 3/8 inch diameter pivotal shaft incorporates two strain gage balances for moment and drag measurement. The lower end of the pivotal shaft could be attached to the rotating arm of a wire wound potentiometer for recording the instantaneous angular position. In addition, means were provided for locking the pivotal shaft in any position; this was used when recording the moment on the container model alone and the container and parachute models in combination.

The A-22 Container models, the parachute models, the moment and force balances, and the angle measuring devices are described in the following paragraphs.

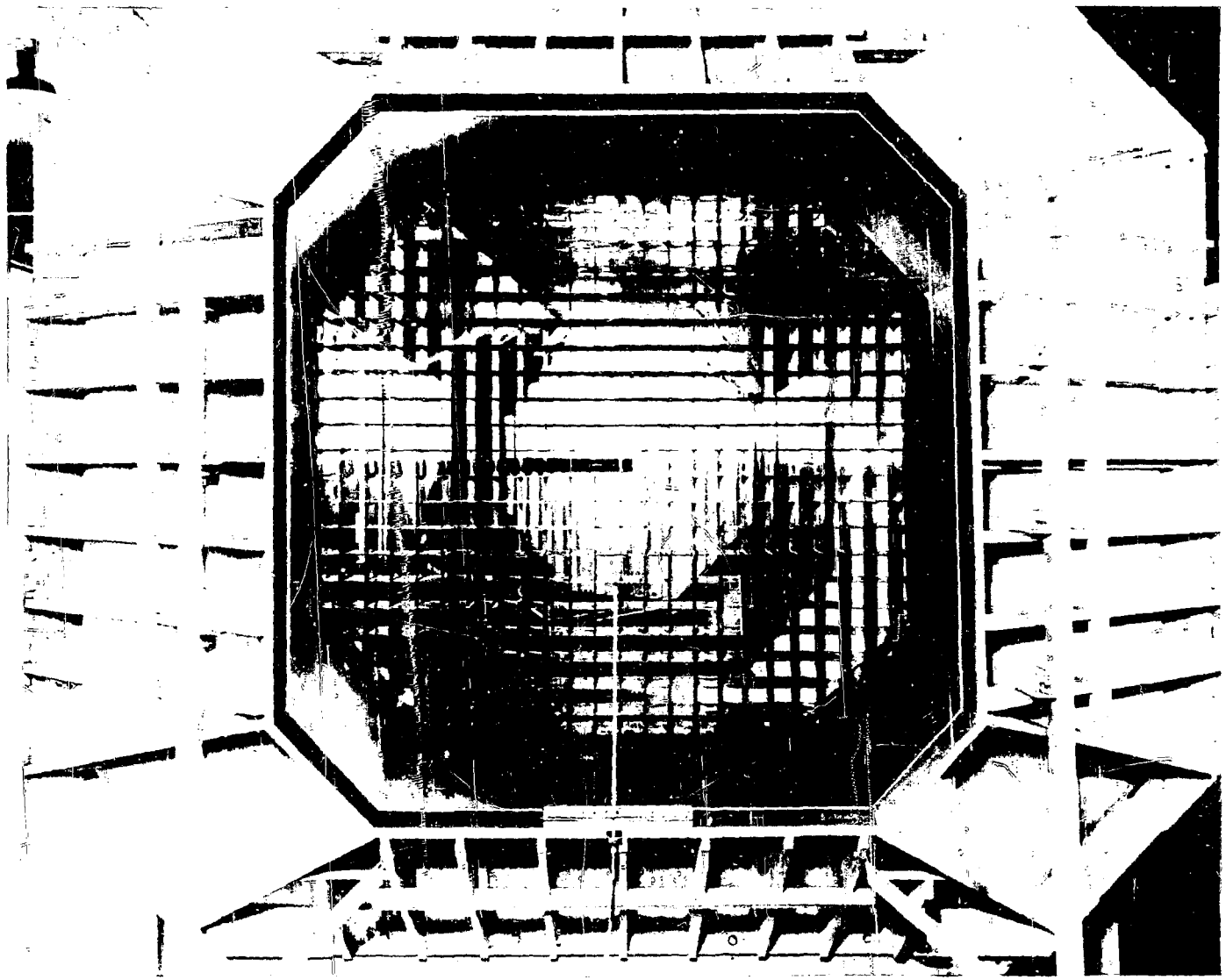

FIG. 2-VIEW FROM OPEN TEST SECTION LOOKING TOWARDS HONEYCOMB INSTALLED UPSTREAM OF NOZZLE ASSEMBLY

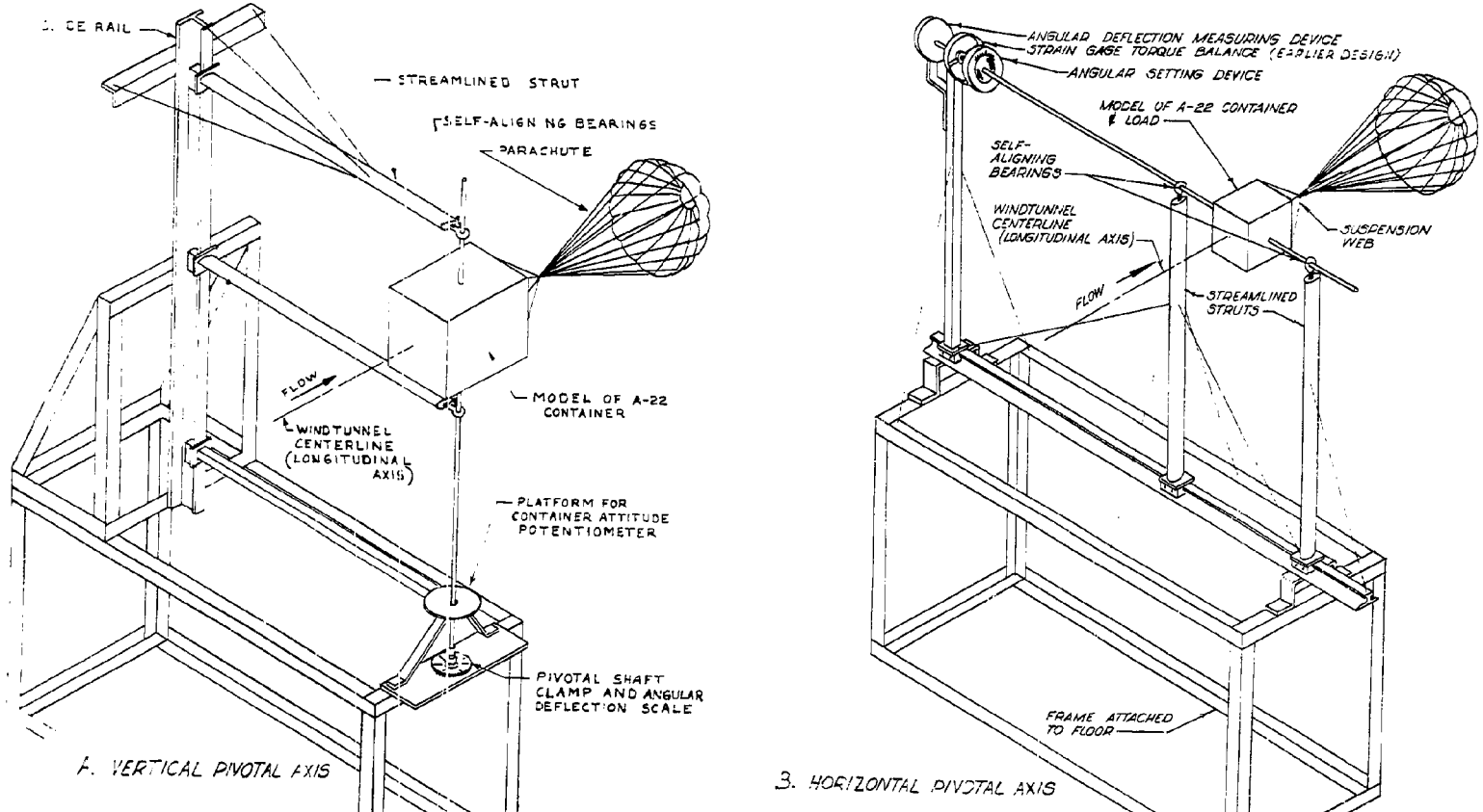

FIG. 3 - PICTORIAL VIEW OF FRAME AND MODEL MOUNTING IN OPEN TEST SECTION

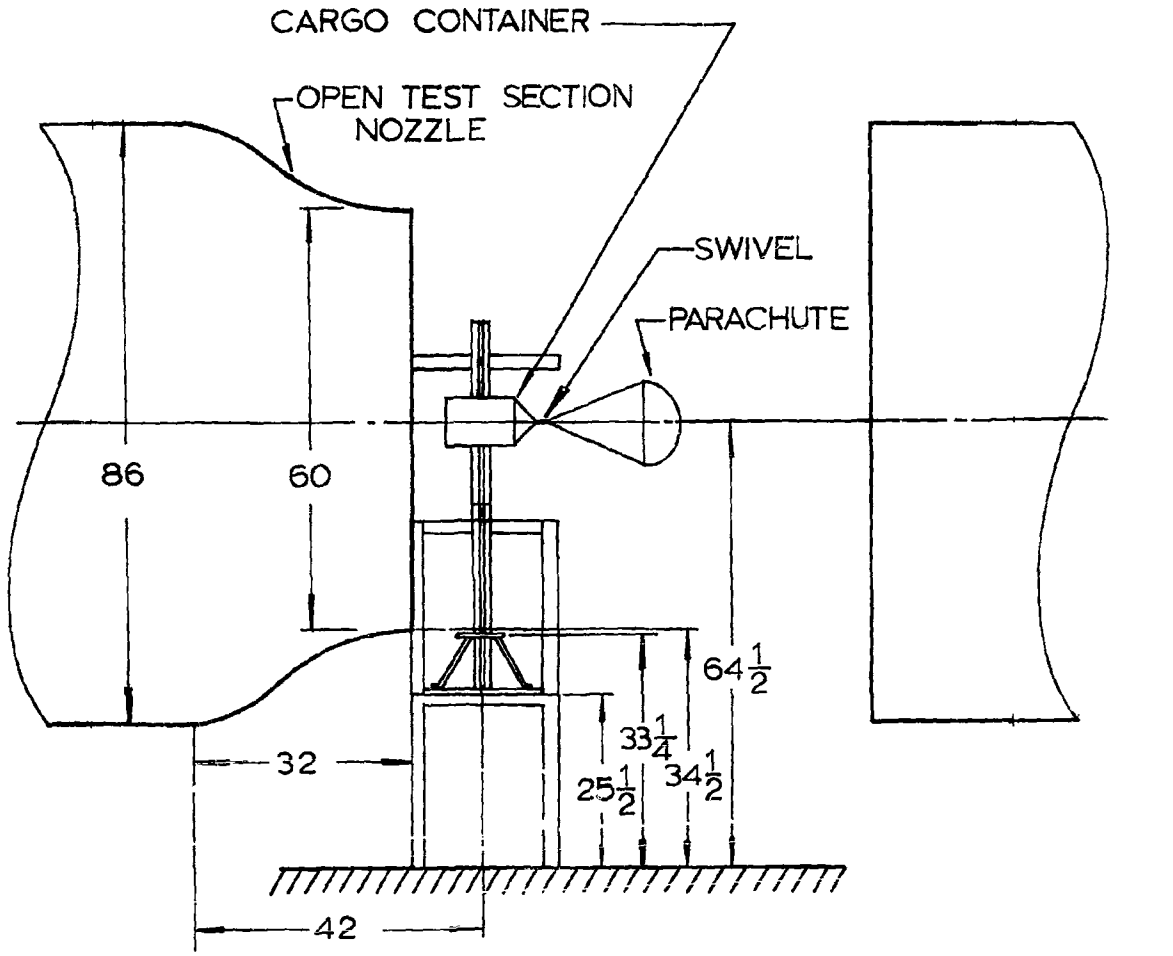

FIG. 4 - GENERAL LAYOUT OF MODEL IN WIND TUNNEL

2.3 A-22 Container Models

Each container model has a central brass fitting into which the two halves of the pivotal shaft can be fitted and anchored as shown in Fig 5.

Orthogonal to the pivotal shaft is a steel threaded shaft which holds steel plates, representing the container base and top. The plates can be arranged at various distances to each other to represent various container heights and various relative positions of the pivotal axis with respect to the top and bottom faces of the container which measure simulates different center of gravity locations of the container. Figure 5 shows design details of the 1/6 scale A-22 Container model.

2.4 Parachute Models

The experimental tests involved parachute canopy models of the following types:

1) Solid flat canopy
2) Ring slot, 20% porosity canopy
3) Ribbon, 20% porosity canopy
4) Ribless guide surface canopy.

The first type (solid flat) was used for purposes of comparison and reference.

The parachute model specifications are given in Fig 6.

(See page 10)

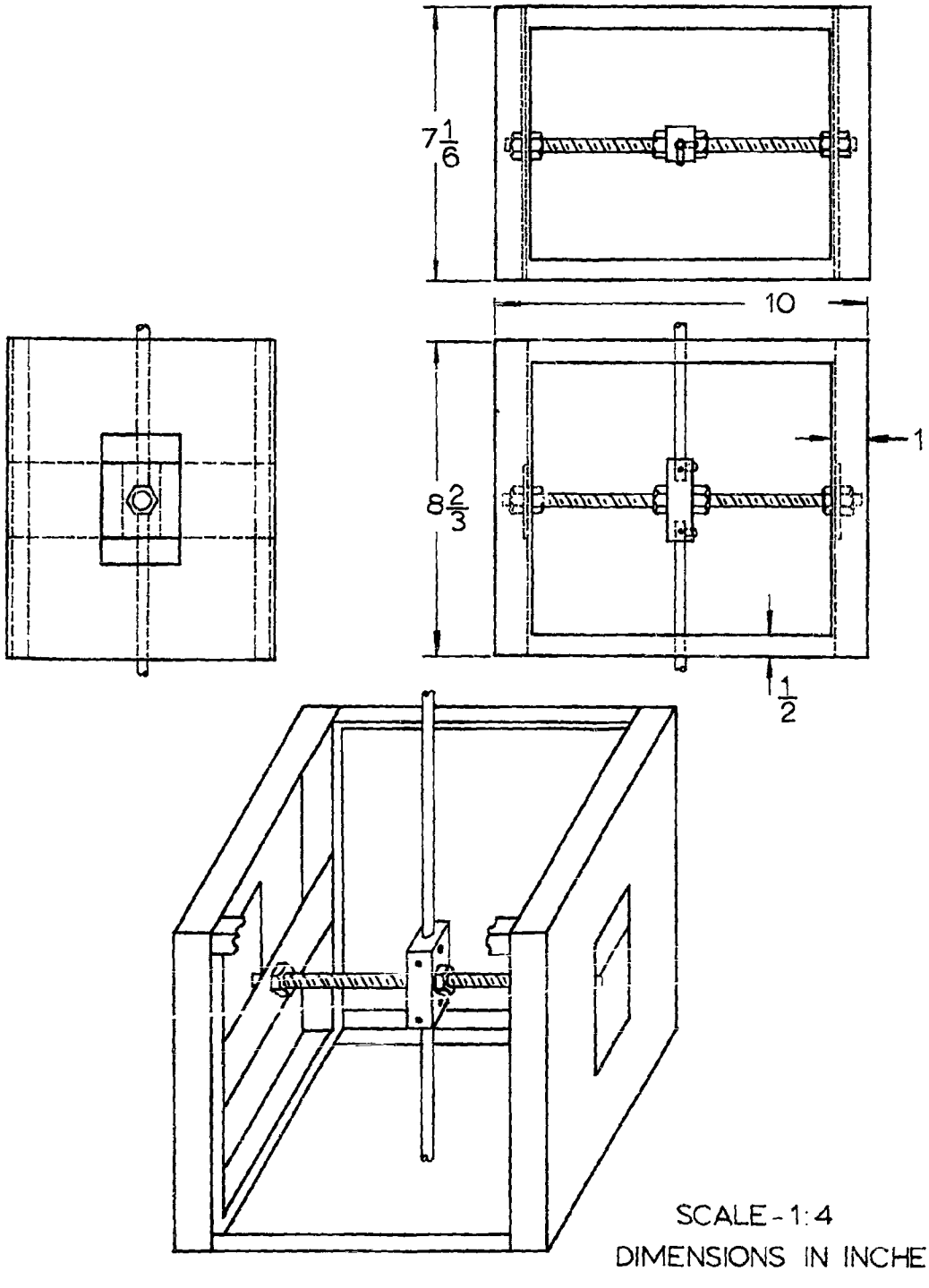

FIG. 5 - DETAILS OF 1/6 SCALE A-22 CONTAINER MODEL FRAME

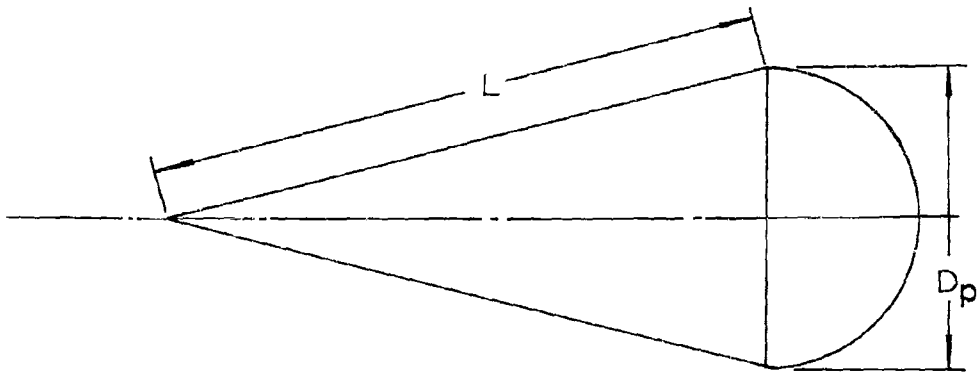

L = length of suspension lines; D_p = projected diameter; D_o = nominal diameter; S_p = projected area; S_o = cloth area; and W = parachute model weight.

MODEL TYPE	L (in.)	D_p (in.)	D_o (in.)	S_p (ft^2)	S_o (ft^2)	W (oz.)
Solid Flat	16.0	- -	16.0	- -	1.452	0.854
Ring Slot, 20% Porosity, 100" prototype	16.5	- -	16.0	- -	1.396	1.119
Ribbon, 20% Porosity 100" prototype	17.0	- -	16.0	- -	1.396	1.244
Ribless Guide Surface	16.0	11.84	- -	0.765	- -	0.620

FIG. 6— PARACHUTE MODEL SPECIFICATIONS.

Three geometrically similar models of the A-22 Container were used in conjunction with a single parachute model of each type. This procedure was preferred to the other alternative of using one container model and three parachute sizes, since container models are less expensive and easier to manufacture than parachute models. Furthermore, the use of parachute models of different sizes would involve dynamic behavior such as natural frequency, period of oscillation, parachute weight,

etc., which might complicate the analysis. On the basis of the three scales of 1/8, 1/6, and 1/4 and the model parachutes used, as specified in Fig 6 the corresponding full scale parachutes would have projected diameters, D_p, of 96, 72, and 48 in., respectively, for the ribless guide surface and flat diameters, D_o, of 128, 96, and 64 in. for the solid flat, ribbon, and ring slot parachutes. These relative sizes are also presented in Fig 7.

	MODEL CONTAINER SCALE		
	1/4	1/6	1/8
Solid Flat, D_o (in.)	64	96	128
Ring Slot, D_o (in.)	64	96	128
Ribbon, D_o	64	96	128
Ribless Guide Surface, D_p (in.)	48	72	96

FIG. 7 - FULL SCALE PARACHUTE DIAMETERS CORRESPONDING TO THE PARACHUTE MODELS AND DIFFERENT SCALE CONTAINERS

Figure 8 illustrates a container parachute combination in 1/8 scale (full size parachute 96 in. diameter) and the 1/4 and 1/6 scale container models.

The designation by scale is an indirect way of indicating the size of parachute corresponding to the A-22 Container; this is obtained by dividing the parachute model diameter by the scale factor.

The scale was a convenient way of setting up the experiments and classifying the results; however, to make the

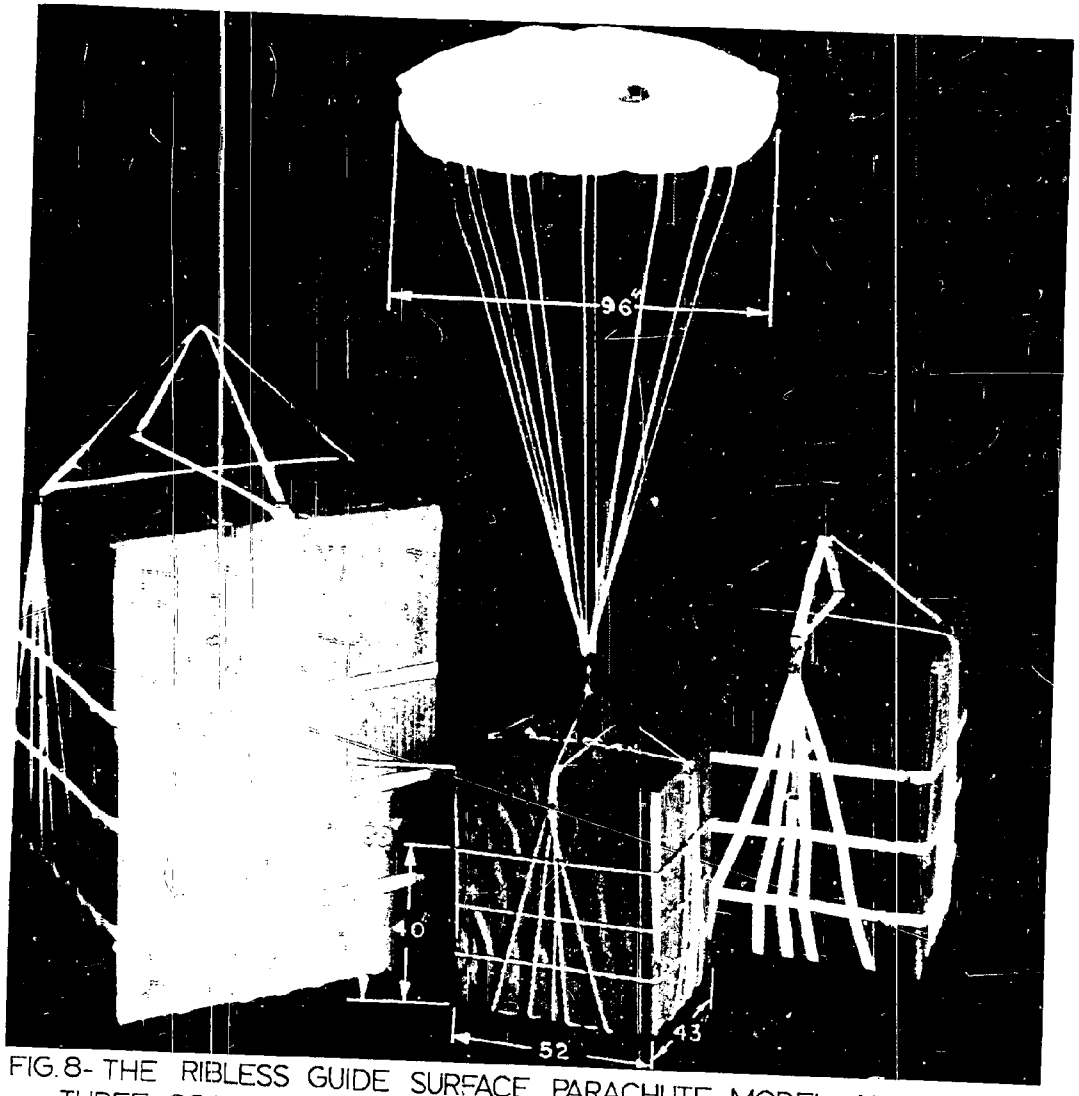

FIG. 8- THE RIBLESS GUIDE SURFACE PARACHUTE MODEL AND THE THREE SCALE MODELS OF THE A-22 CONTAINER (DIMENSIONS REFER TO A FULL SIZE COMBINATION)

presentation of results of more immediate physical significance, we will present the test results in terms of the full scale parachute diameters corresponding to each test configuration.

2.5 Strain Gage Moment Balance

An earlier design of a moment balance proved unsatisfactory, and a different design using the torque tube principle was then constructed and calibrated. The general arrangement and main details of the moment balance are illustrated in Fig 9.

The upper end of the lower half of the 3/8 in. diameter pivotal shaft was drilled out to a wall thickness of 0.030 in. and a depth of 2.75 in., and a 0.75 in. long steel plug was driven into the drilled rod to seal off the end and form a hollow section 2 in. long to serve as the torque tube. Four Baldwin SR-4 type A-7 strain gages were cemented to the tubular section along two orthogonal but not intersecting helical paths on the surface of the torque tube and connected as a 4-arm bridge circuit.

The pivot shaft was then remounted in bearings on the test frame with the torque tube end passing into the brass fitting of the model container and locked in place with two set screws. The strain gages are thus located inside the container model where they are protected from mechanical damage.

Figure 10 illustrates the calibration curve of the moment balance.

2.6 Strain Gage Drag Balance

A strain gage drag balance was constructed as an integral

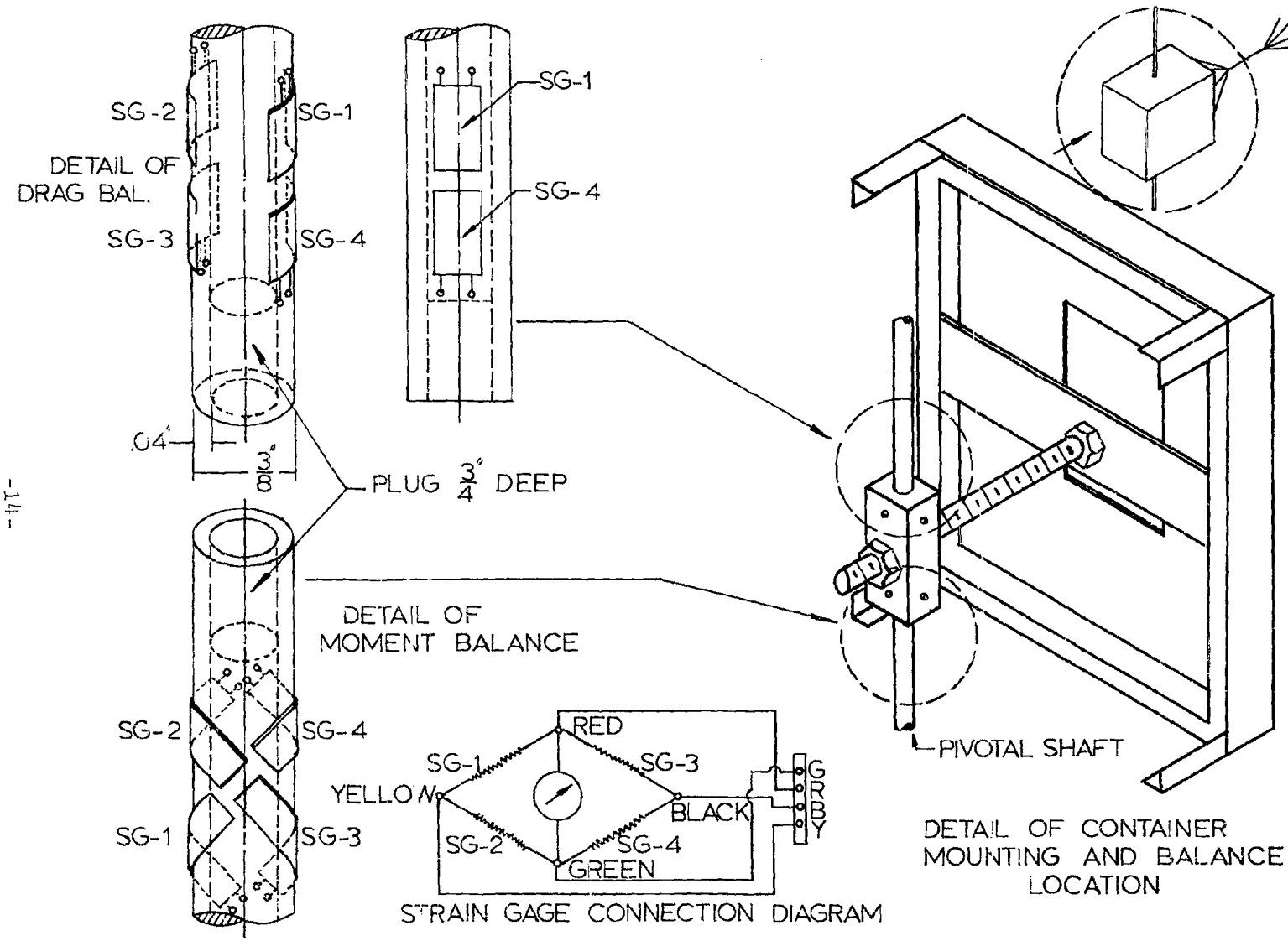

FIG. 9 - GENERAL ARRANGEMENT AND DETAIL OF MOMENT AND DRAG BALANCES

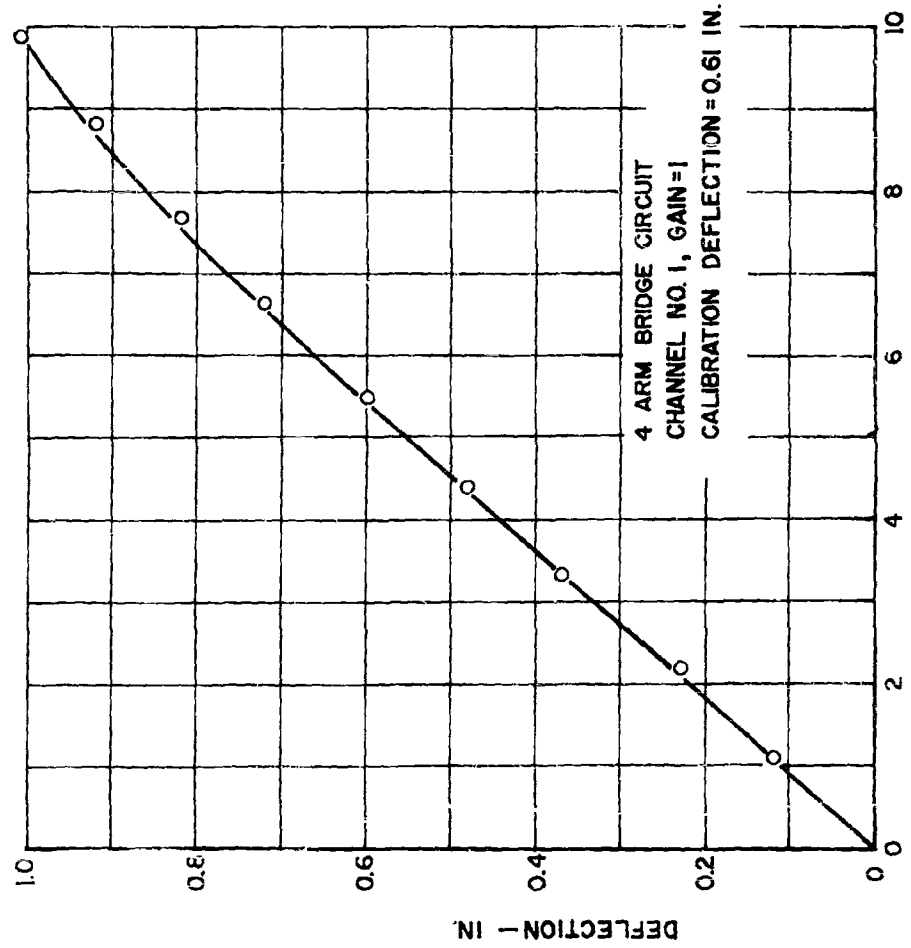

FIG. 10- MOMENT BALANCE CALIBRATION

part of the upper section of the pivotal shaft. For this purpose, the end of the pivotal shaft which fits into the brass fitting within the container model was drilled to a depth of 2.75 in. leaving a wall thickness of 0.040 in. Strain gages were then cemented along the axis of the shaft, two on each side of the hollowed section, and the four strain gages were electrically connected as a 4-arm bridge. The pivot shaft was then re-installed on the test frame with the drag balance end passing into the container brass fitting and secured with set screws.

The general arrangement of the drag balance and its main dimensions are illustrated in Fig 9, and its calibration curve is presented in Fig 11.

2.7 Attitude Measuring Devices

2.7.1 Container Angle Measuring Device

The device is essentially a wire wound potentiometer mounted at the lower end of the pivotal shaft with the potentiometer wiper locked to the pivotal shaft to record the instantaneous angular position of the container's longitudinal axis with respect to the air stream.

The potentiometer has 1020 turns over an arc of 340 degrees, i.e., the angular resolution is 1/3 of 1 degree. The potentiometer was connected in a two-arm bridge circuit. Figure 12 gives the static calibration curve which indicates satisfactory sensitivity and linearity.

2.7.2 Parachute Angles Measuring Device

A special device for measuring the parachute attitude

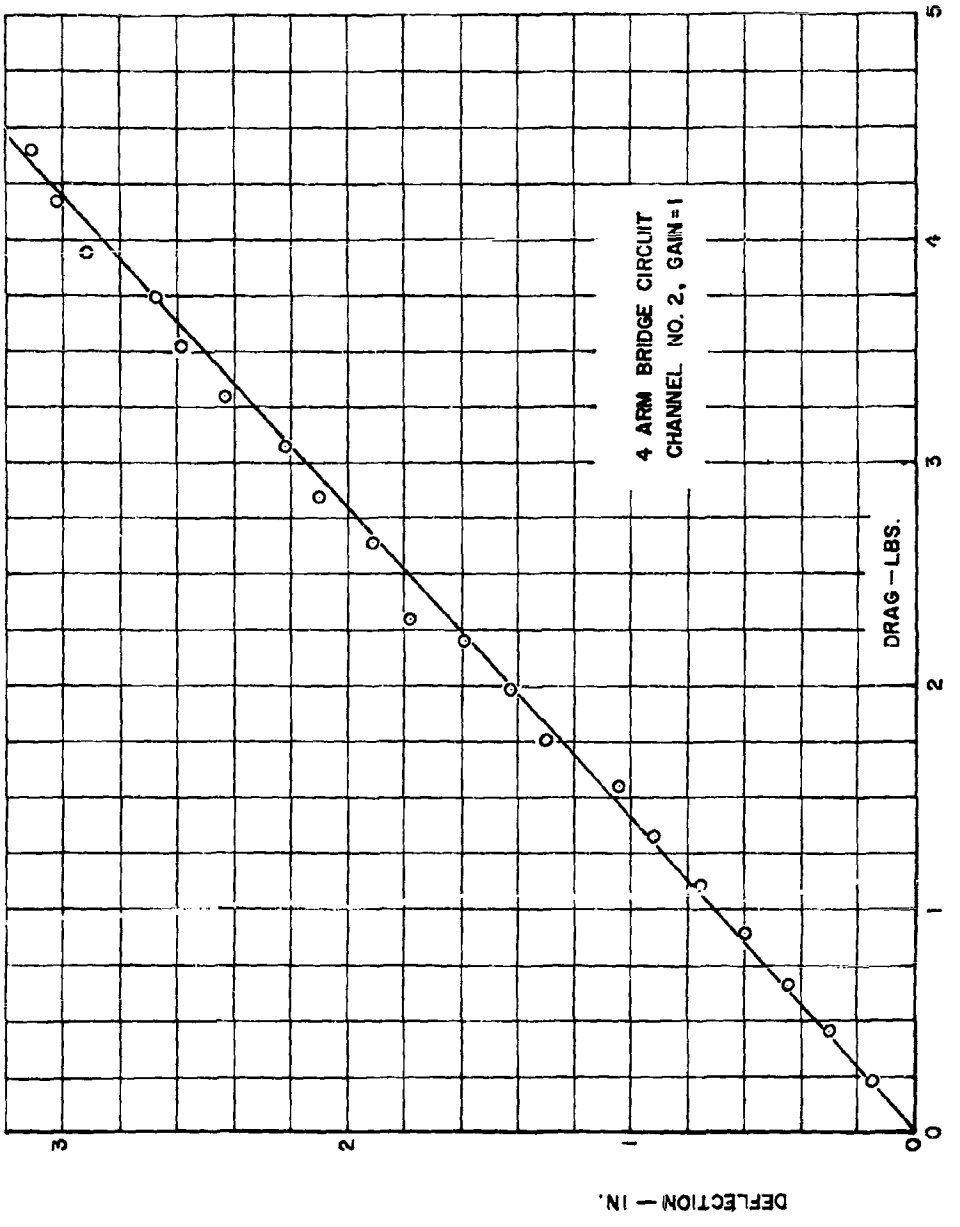

FIG. 11- DRAG BALANCE CALIBRATION

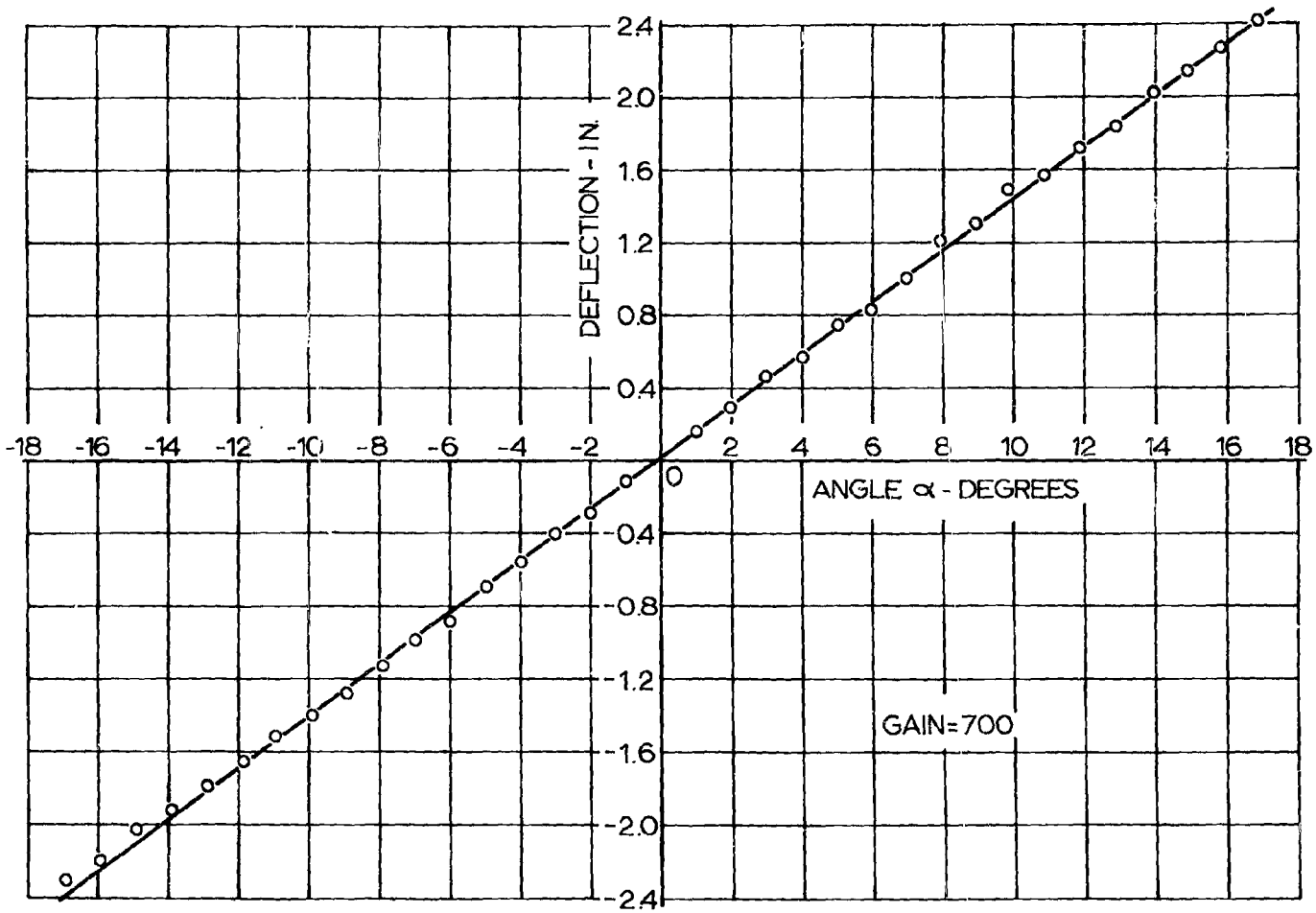

FIG. 12 - CONTAINER ATTITUDE ANGLE CALIBRATION CURVE

angles was constructed and is illustrated in Figs 13 and 14.

It has, on one side, a rigid cross frame with four pick-up points which are hinged to the four lines forming the A-22 Container model suspension web (spider) and on the other side, an axial arm which engages the clevis assembly of the parachute model.

This attitude measuring device provides free pivoting about two orthogonal axes and, when the device is in its neutral position, i.e., when the longitudinal axis of the container and that of the parachute coincide with the direction of airflow, the pivoting axes are respectively horizontal and vertical and both lie in a plane perpendicular to the direction of airflow.

The angular motions about each of these two axes are transmitted to the wipers of two miniature potentiometers. Each potentiometer forms the variable arms of a two-arm bridge circuit. One of the potentiometers picks up the angle of yaw (Angle θ) while the other is sensitive to the angle of pitch (Angle ψ) of the parachute axis with respect to the container's longitudinal axis.

Calibration of the two miniature potentiometers is given in Figs 15 and 16. These potentiometers have a carbon ring as the resistance element and, because of the severe limitations of size, their linearity is not as good as that of the large wire-wound type used on the container pivotal axis but it is acceptable.

2.8 Parachute Risers

Initial tests to determine the moment coefficients and

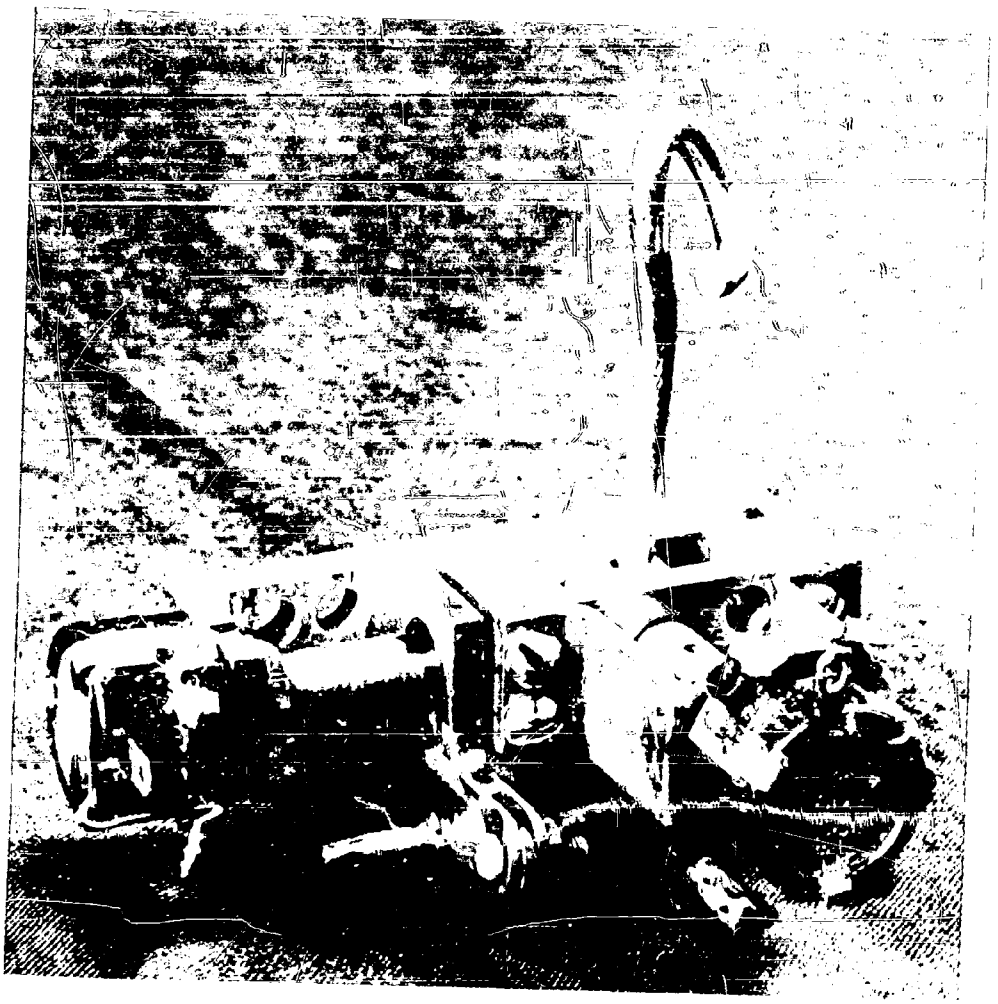

Figure 13. Parachute Attitude Measuring Device

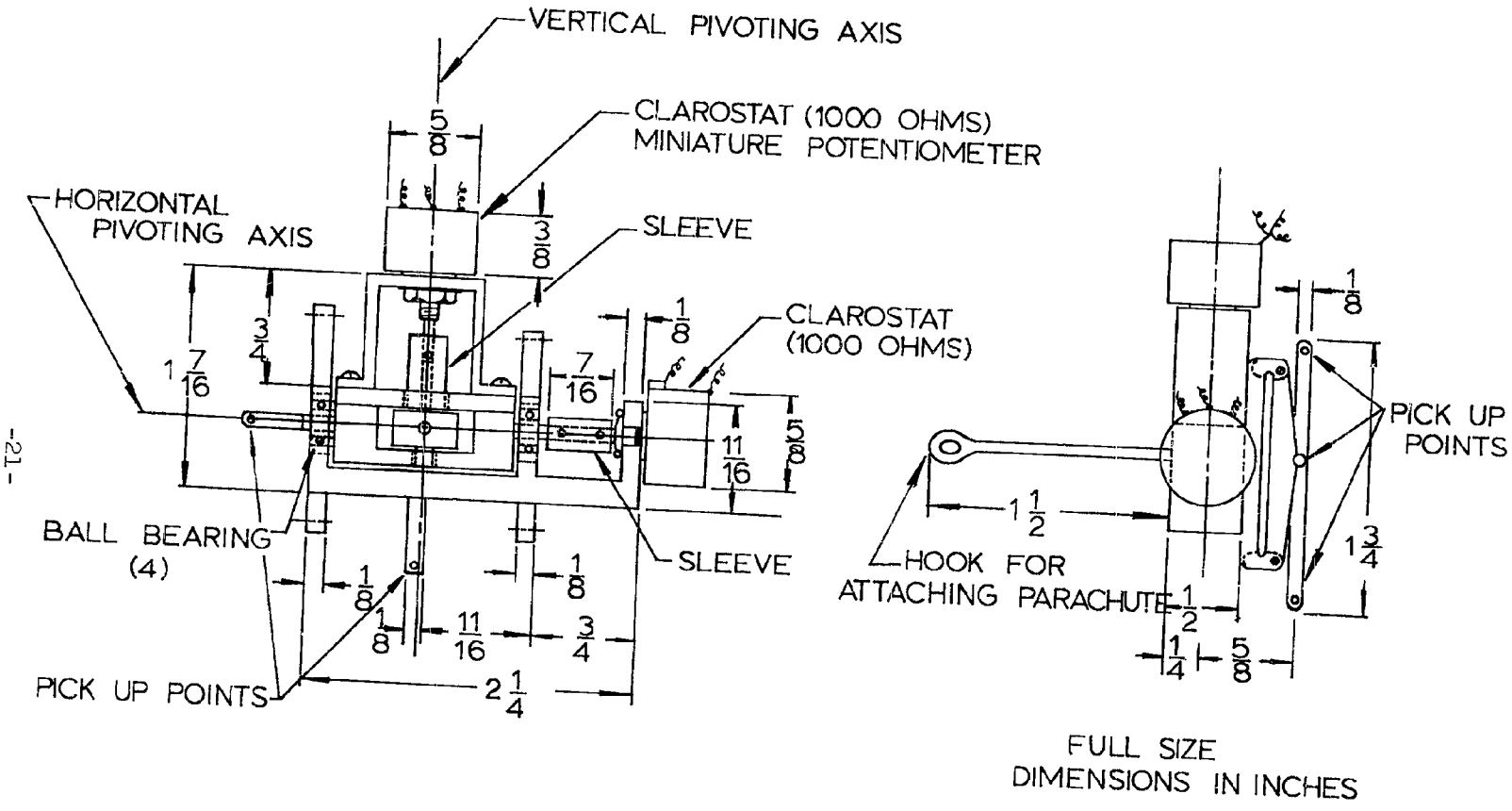

FIG. 14- PARACHUTE ATTITUDE MEASURING DEVICE-DESIGN DETAILS AND DIMENSIONS

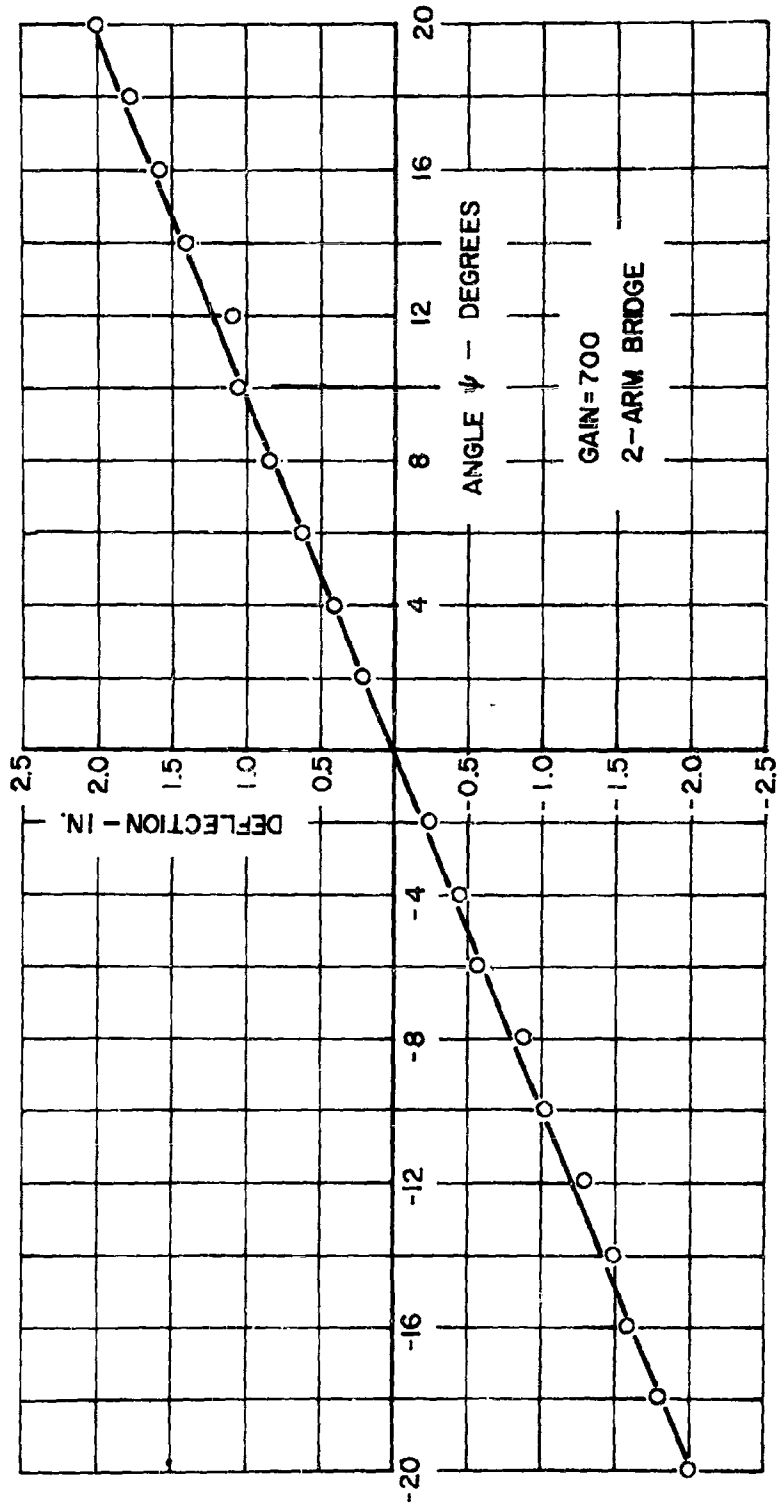

FIG. 15- PARACHUTE ATTITUDE CALIBRATION CURVE - ANGLE ψ

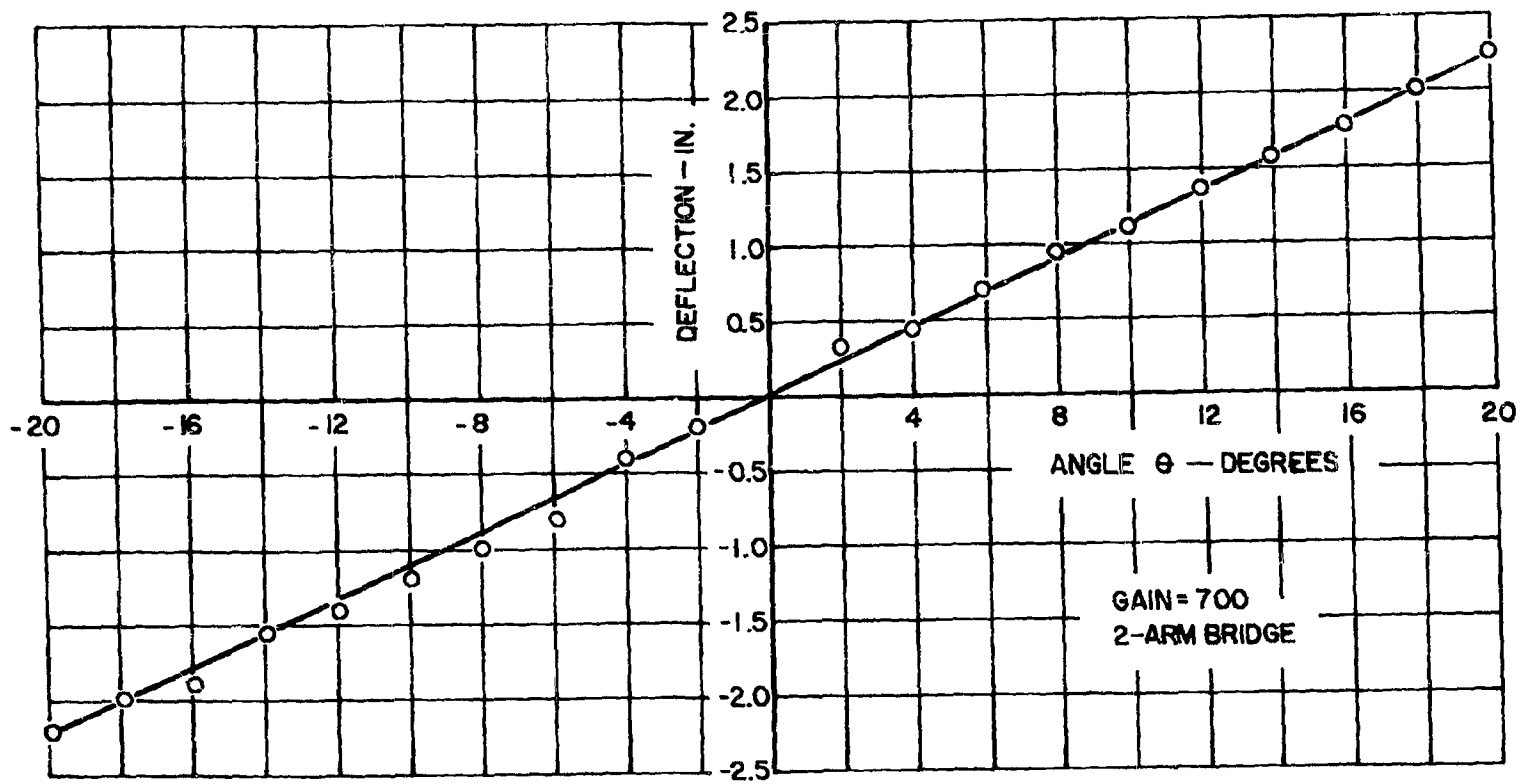

FIG. 16 - PARACHUTE ATTITUDE CALIBRATION CURVE - ANGLE θ

the free attitude angles were conducted without risers.

In actual aerial delivery, a riser is interposed between the container spider web and the parachute suspension lines. Tests representing the 72 in. and 48 in. guide surface parachutes and the 96 in. and 64 in. solid flat, ribbon, and ring slot parachutes were conducted with various riser lengths up to and including scaled riser lengths representing 30 ft full scale.

III. EXPERIMENTAL PROCEDURE AND RESULTS

3.1 System of Reference

It is convenient to specify a system of three orthogonal axes with its origin at the C. G. position of the container. The first axis, the longitudinal axis, may be defined as the axis through the C. G. perpendicular to the base of the container, i.e., in the height direction. The other two axes through the C. G., the lateral axes, are orthogonal to the longitudinal axis. One may consider an infinite number of such orthogonal lateral axes but, since the spider web attaches at the mid-points of the rectangle forming the top surface, it is natural to consider the system of two lateral axes that are perpendicular to the side faces of the container. Figure 17 illustrates the reference system used, gives the notation for the container, and parachute attitude angles, and indicates the critical orientation for the pivotal axis, the reference area, and the characteristic length used in the aerodynamic calculations.

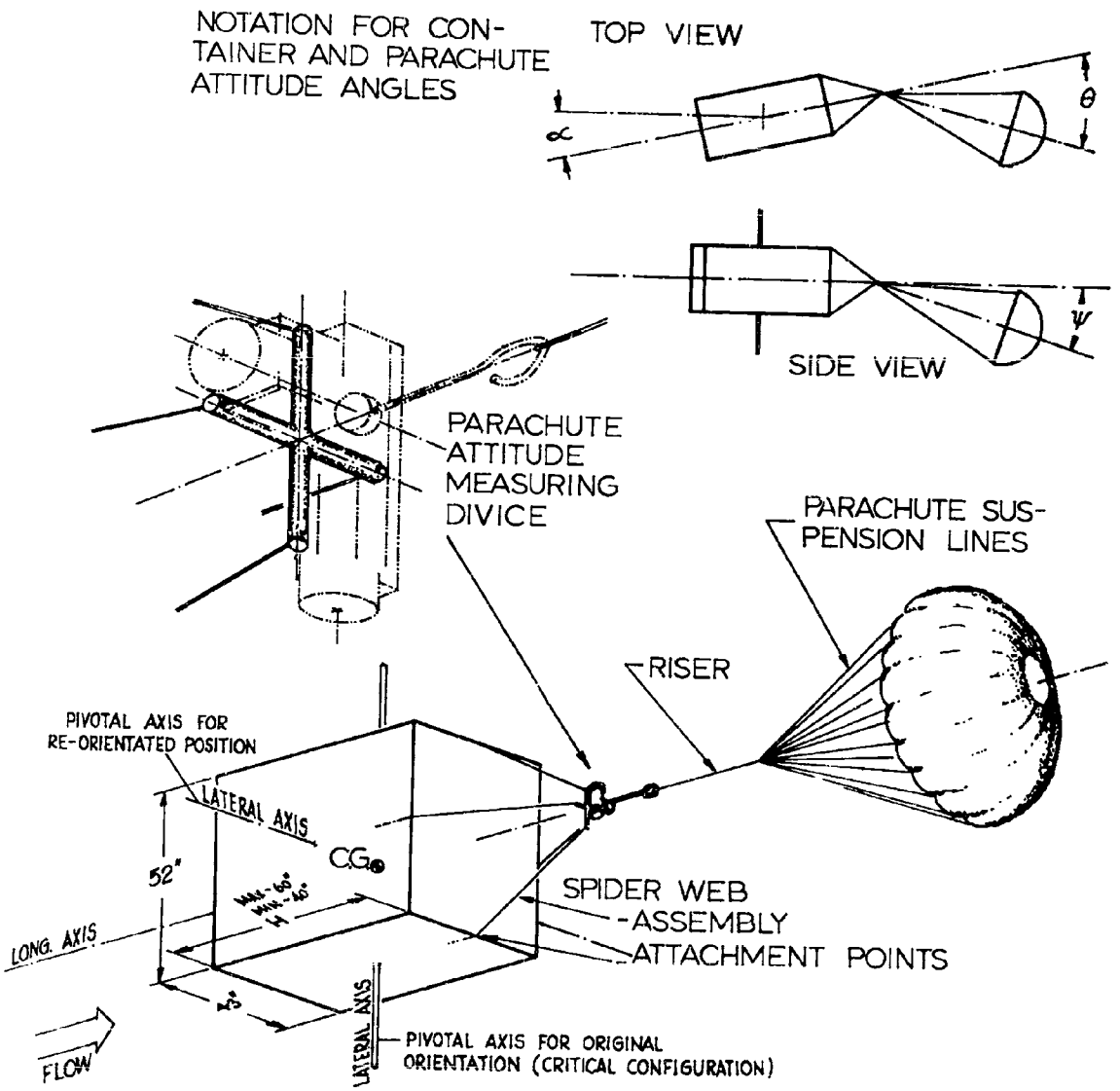

CONTAINER BASE AREA
43" × 52" = 2236 in^2 (REF. AREA)
BASE DIAGONAL
67.48 in (CHARACT. LENGTH)

FIG. 17 SYSTEM OF REFERENCE

3.2 Test Reynolds Numbers

All the tests presented in this report were conducted at a dynamic pressure setting of q = 5.20 lb per sq ft corresponding to an air speed of 67.6 ft per sec and a water head of 1 inch. Throughout the testing, the pressure head was accurately controlled by means of a Meriam Micromanometer with a sensitivity of 0.001 inch of water.

The reference area used for calculating the aerodynamic coefficients was the container base area and the characteristic length used for calculating the moment coefficient and the Reynolds number was the diagonal of the container base. On the basis of this characteristic length and the other experimental conditions, the corresponding Reynolds numbers for the different scales were as follows:

$Re = 2.75 \times 10^5$ for the 1/8 scale container

$Re = 3.66 \times 10^5$ for the 1/6 scale container

$Re = 5.49 \times 10^5$ for the 1/4 scale container.

3.3 Critical Container Configurations

3.3.1 Critical Container Orientation

Since the container base is not square but rectangular, it was necessary to determine the critical container orientation, i.e., the one producing the largest de-stabilizing moments. For this purpose, tests were conducted with the 1/6 scale container model mounted on the test frame in the two possible orientations and the moments were measured through the full range of angles.

The results are illustrated in Fig 18 from which it is seen that the original position is the more critical and this orientation was therefore used for all subsequent tests.

3.3.2 Critical Container Height

Since the container height is variable, depending on the nature of the load, tests were conducted with container models representing the two extreme values of the height corresponding to maximum and minimum heights (respectively 60 and 40 inches full scale). Figure 19 gives the result of these tests indicating that the maximum height configuration has the more critical stabilization requirements, i.e., smaller stable range and stable moment coefficients in that range and larger de-stabilizing moments beyond it. The maximum height configuration was therefore used in all the later tests.

3.4 Tests with Container Model Alone

3.4.1 Moment Characteristics

Each of the three container models (1/8, 1/6, and 1/4 scale) was successively mounted on the test frame, statically balanced, and carefully positioned. The zero angle of attack was selected at the position where the resulting galvanometer deflection, i.e., the moment coefficient was zero. This adjustment was necessary because the airflow is slightly non-symmetrical in the secondary test section of the wind tunnel. The moments were then recorded in two degree increments for α in the range from 0 to $\pm$ 20 degrees and in five degree increments from $\pm$ 20 to $\pm$ 90 degrees.

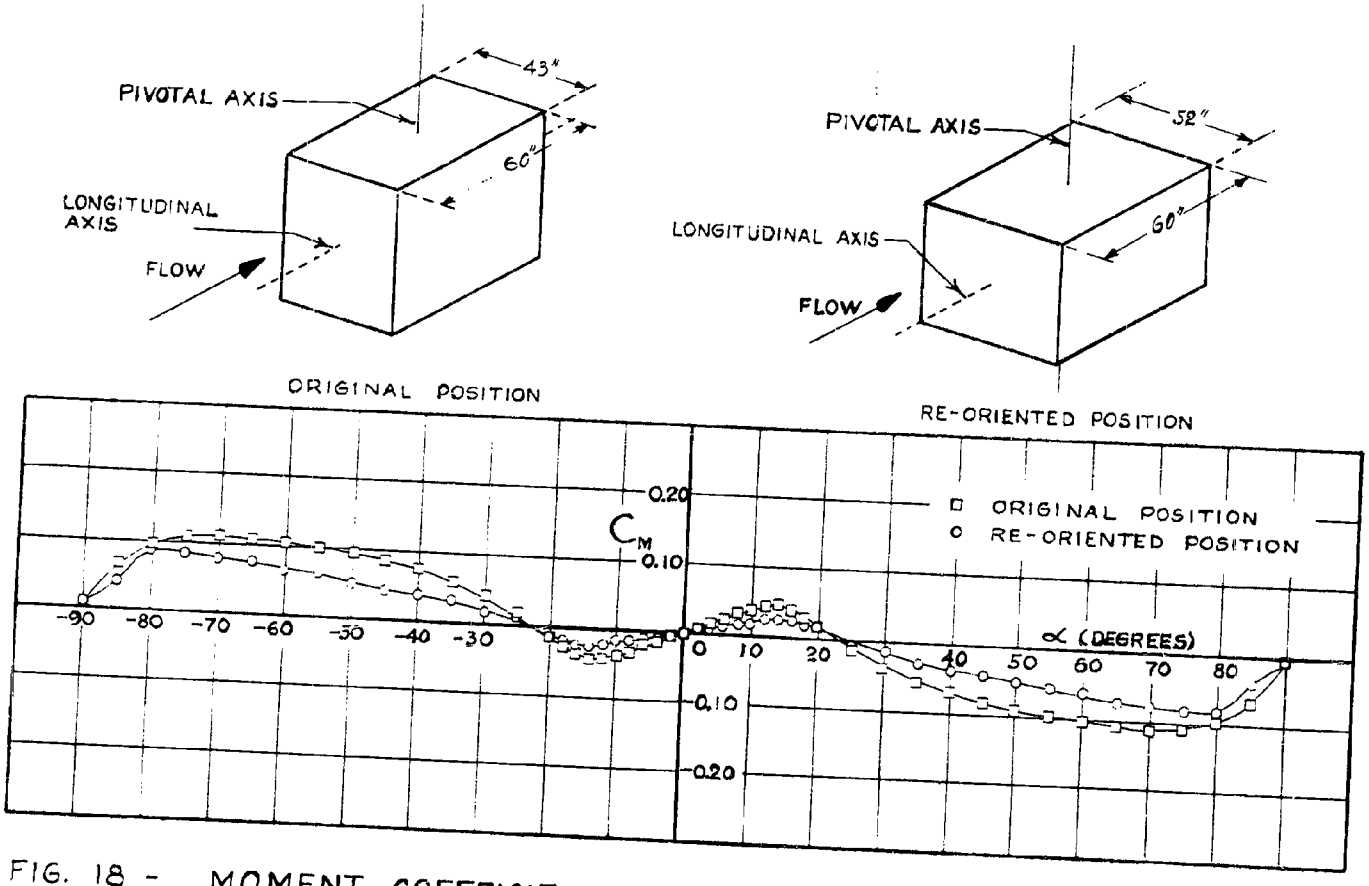

FIG. 18 - MOMENT COEFFICIENT FOR A-22 CONTAINER MODEL ALONE IN ORIGINAL AND RE-ORIENTED POSITIONS

REYNOLDS NO = 3.66×10^5

CONTAINER DIMENSIONS : $10" \times 8\frac{2}{3}" \times 7\frac{1}{6}"$

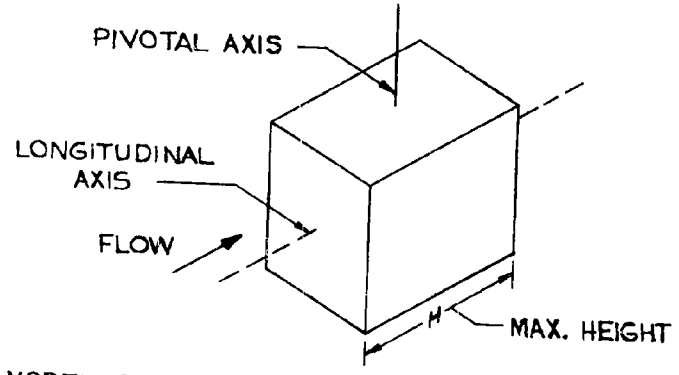

MODEL CONTAINER DIMENSIONS:
HEIGHT: 10.0 IN. BASE: 8.67x 7.17 IN.
1/6 FULL SCALE

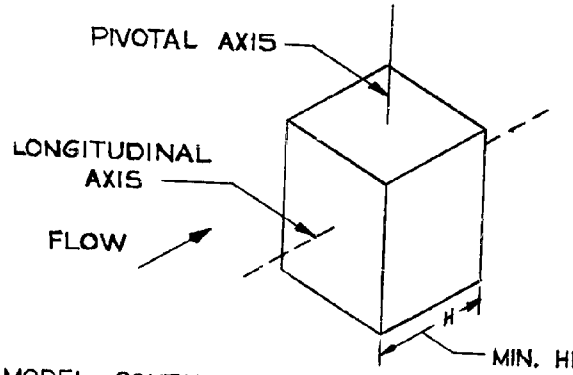

MODEL CONTAINER DIMENSIONS:
HEIGHT: 6.67 IN. BASE: 8.67 x 7.17 IN.
1/6 FULL SCALE

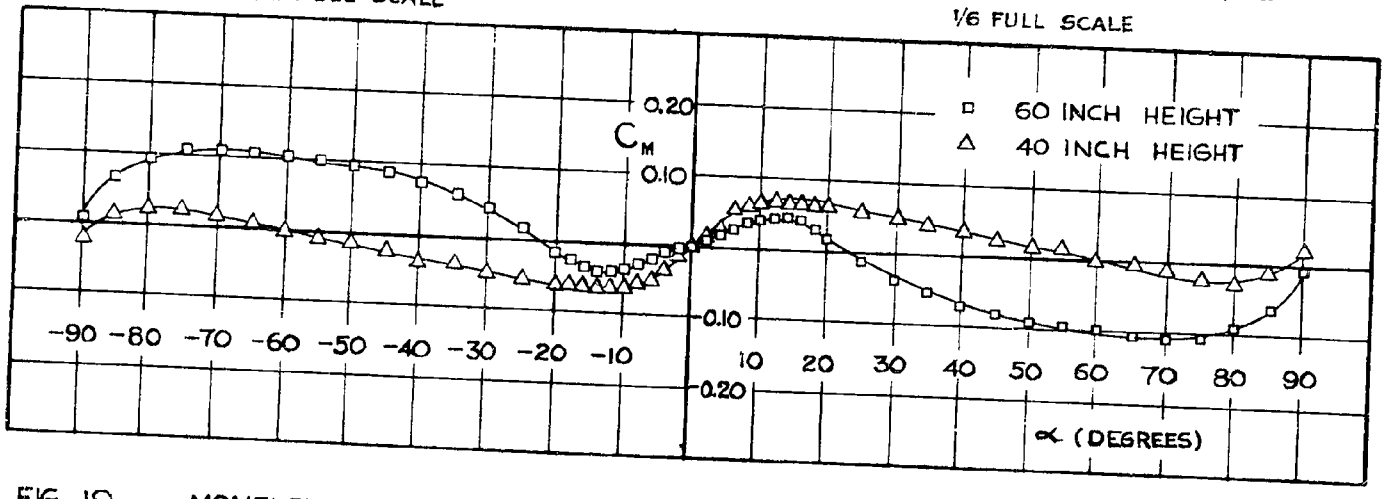

FIG. 19 - MOMENT COEFFICIENT OF A-22 CONTAINER MODEL REPRESENTING 60 IN. AND 40 IN. FULL SCALE CONTAINER HEIGHTS
TEST REYNOLDS NO. = 3.66×10^5

The moment coefficient versus the angle of attack for the three scale container models alone are presented in Fig 20. This figure indicates that the container alone is stable in a range of about ± 25 degrees. Beyond that range, it is unstable.

Comparison of the moment coefficients for the three geometrically similar scale models of the container indicate the same general shape for the variation of moment coefficient with angle of attack, but with small differences in the numerical values.

3.5 Tests with Parachute Stabilized Container Model Without Risers

3.5.1 Moment Characteristics

After testing each scale model of the container alone, the attitude measuring device was secured to the container web, a parachute model was attached and the system statically rebalanced. The moment characteristics for the system were then recorded in two degree increments for α in the range from 0 to ± 20 degrees and in five degree increments beyond ± 20 degrees. These were repeated for each of the four parachute models listed in Fig 6.

For the configurations representing guide surface parachutes of 96 in. and 72 in. diameter and parachutes of 128 in. and 96 in. for the other three types, the angular range without risers was limited to ± 45 degrees.

For the configurations representing a 48 in. guide surface parachute and 64 in solid flat, ribbon, and ring slot

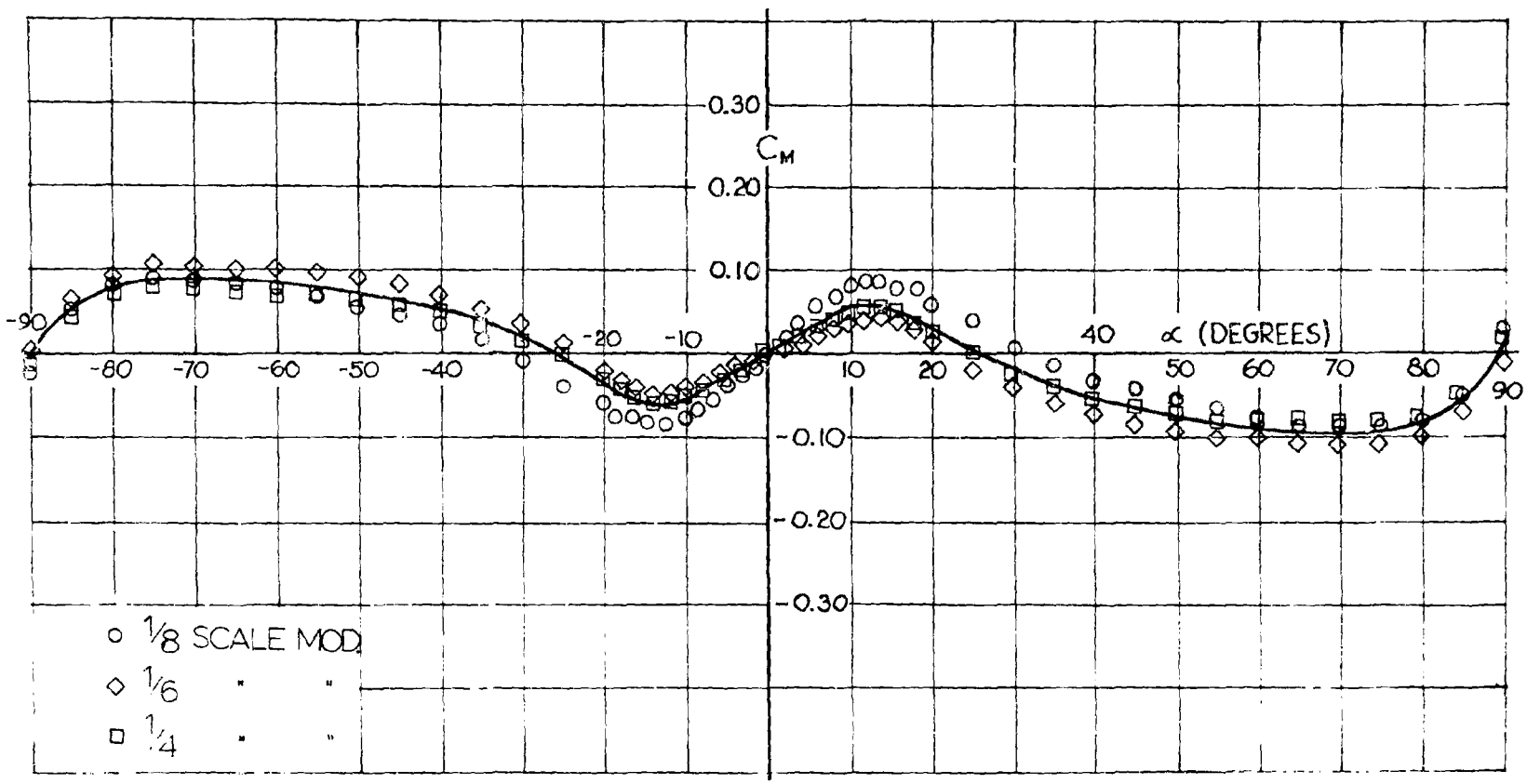

FIG. 20- MOMENT COEFFICIENT FOR THREE SCALE MODELS OF A-22 CONTAINER

parachutes, it was not practical to go beyond $\alpha = \pm 35$ degrees because of the violent parachute motions resulting from the large wake and the fact that some of the spider web lines became slack at large angles.

In all cases, the values obtained for the moment coefficients at identical positive and negative angles of attack were averaged to account for minor flow variations in the test section.

3.5.1.1 Tests with Parachute Models Representing Solid Flat, Ribbon, and Ring Slot Parachutes of 128 inch Diameter and a Ribless Guide Surface Parachute of 96 inch Diameter

Figure 21-A, B, C, and D present the moment coefficients for the A-22 Container in combination with the four parachute types with no risers.

Figure 21-A shows the moment characteristics for the parachute container configuration representing a solid flat parachute of 128 inch diameter. This configuration exhibits an unstable range of $\pm$ 6 degrees, beyond which it is stable up to the maximum range tested ($\pm$ 40 degrees). Furthermore, the maximum moment coefficient (1.37 at 40 degrees) was the highest of the four configurations tested.

Figure 21-B shows the moment characteristics for the configuration with a 20% porosity 128 inch diameter ring slot parachute it exhibits an unstable range of $\pm$ 4 degrees, beyond which it is stable up to the maximum range tested ($\pm$ 45 degrees). The maximum measured value of the moment coefficient was 1.12 at 45 degrees.

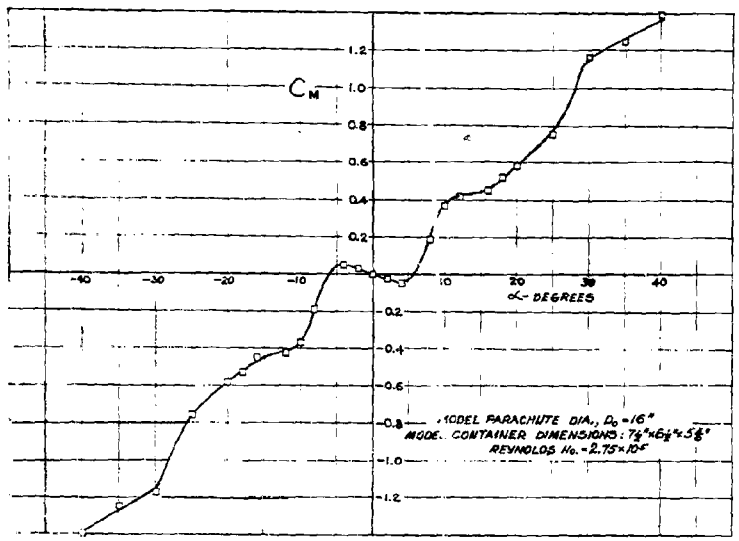

A.- CONTAINER WITH 128" DIA. SOLID FLAT PARACHUTE

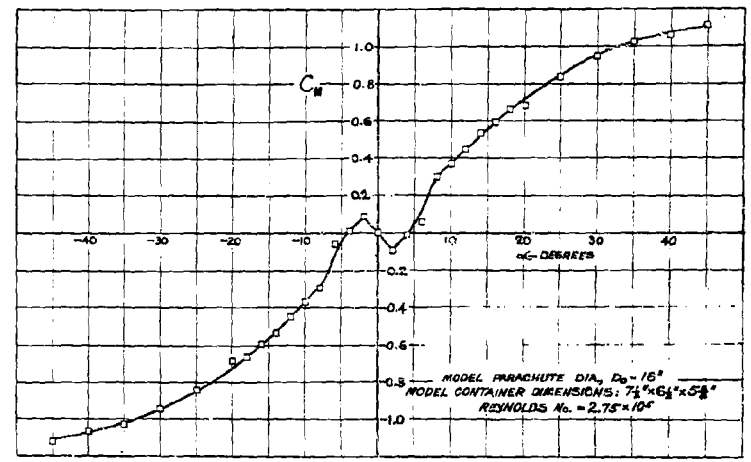

B.- CONTAINER WITH 20% POROSITY 128" DIA. RING SLOT PARACHUTE

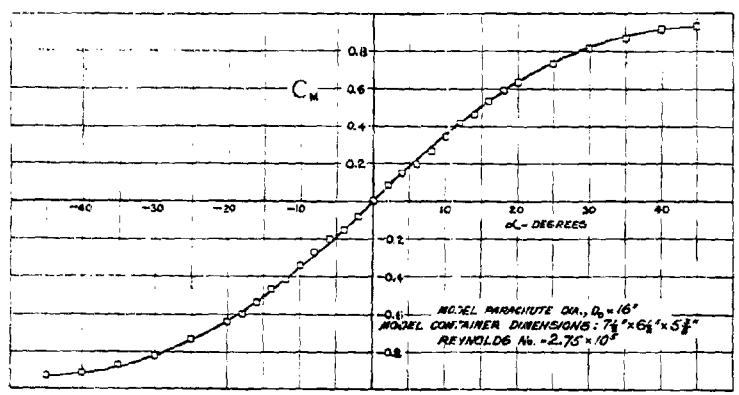

C.- CONTAINER WITH 20% POROSITY 128" DIA. RIBBON PARACHUTE

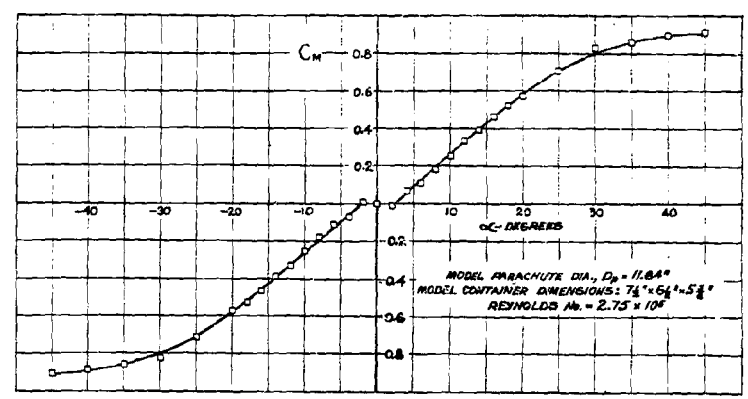

D.- CONTAINER WITH 96" DIA. RIBLESS GUIDE SURFACE PARACHUTE

FIG. 21 - MOMENT COEFFICIENT FOR MODEL SYSTEMS REPRESENTING THE A-22 CONTAINER WITH FOUR PARACHUTE TYPES WITH NO RISERS

Figure 21-C gives the moment characteristics for a parachute container system using a 20% porosity 128 inch diameter ribbon parachute. It indicates that this configuration is stable over the full angular range tested, i.e., $\pm$ 45 degrees. The maximum stabilizing moment coefficient measured was 0.93 at 45 degrees.

Figure 21-D indicates that a 96 inch diameter ribless guide surface parachute would stabilize the container over the full range tested, i.e., $\pm$ 45 degrees. The maximum stabilizing moment coefficient measured was 0.96 at 45 degrees.

Figure 22 presents, for comparison purposes, the moment coefficient versus α for each of the four parachute container configurations given above when used with no risers.

3.5.1.2 Tests with Parachute Models Representing Ribbon and Ring Slot Parachutes of 96 inch Diameter and a Ribless Guide Surface Parachute of 72 inch Diameter

The moment characteristics for the container parachute configuration with the 20% porosity, 96 inch diameter ring slot parachute are shown in Fig 23-A. This combination is found to be stable for all angles of attack tested. The maximum moment coefficient was obtained at $\pm$ 25 degrees, the value being 0.345. This combination had the greatest stabilizing characteristics of the types tested in the region near $\alpha = 0$.

Figure 23-B shows the moment coefficients for the container in combination with the 20% porosity, 96 in. diameter ribbon parachute. This configuration is stable for all measured angles of attack. The maximum moment coefficient was 0.240 at

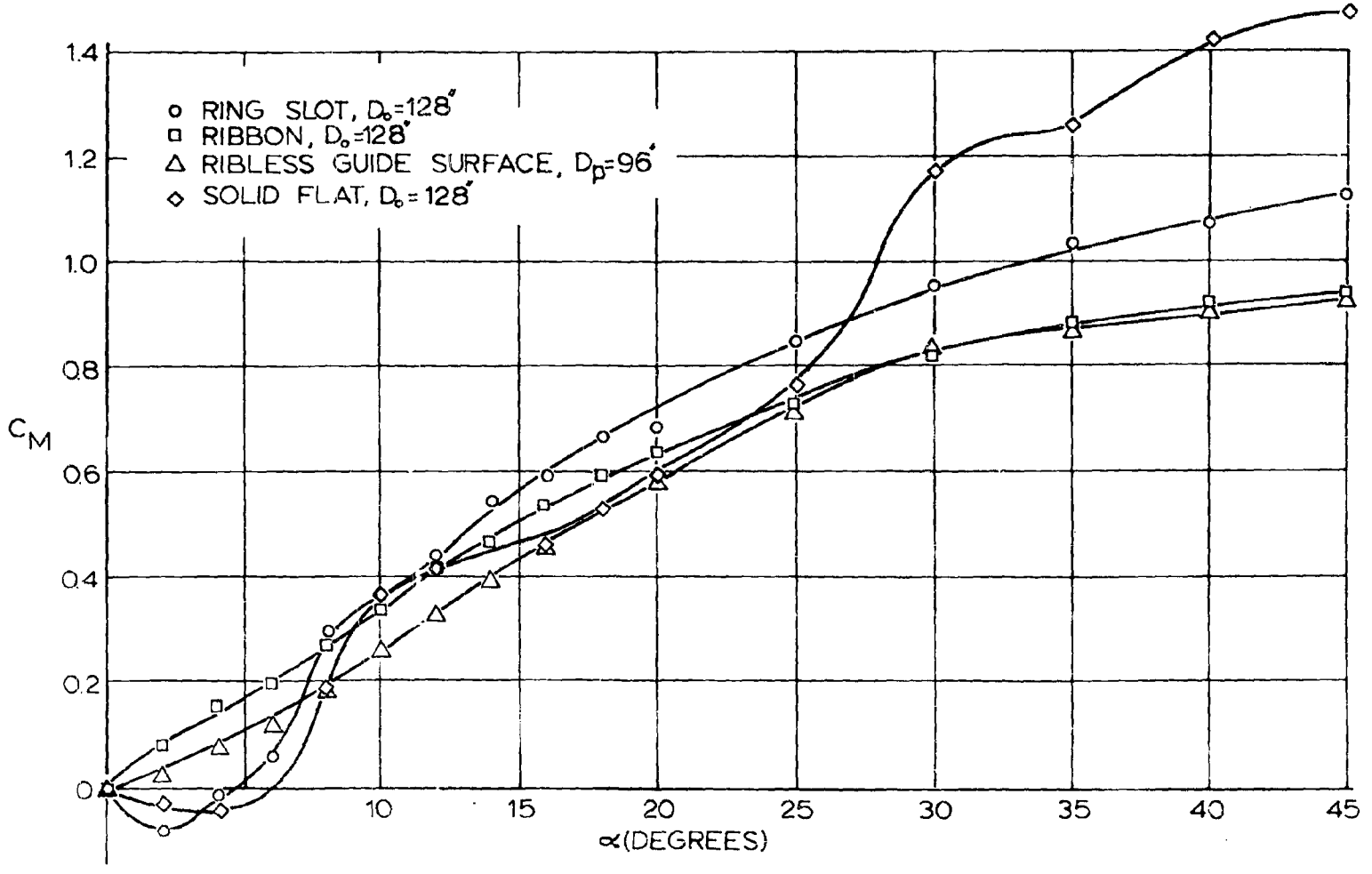

FIG 22-MOMENT COEFFICIENT FOR A-22 CONTAINER AND VARIOUS PARACHUTE MODELS WITH NO RISERS

REYNOLDS NO. = 2.75×10^6 CONTAINER DIMENSIONS $7\frac{1}{2}'' \times 6\frac{1}{2}'' \times 5\frac{1}{8}''$

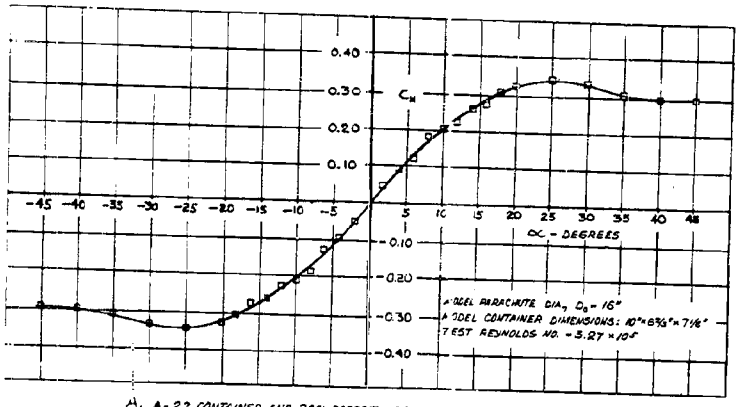

A. A-22 CONTAINER AND 20% POROSITY 96" DIA. RING SLOT PARACHUTE

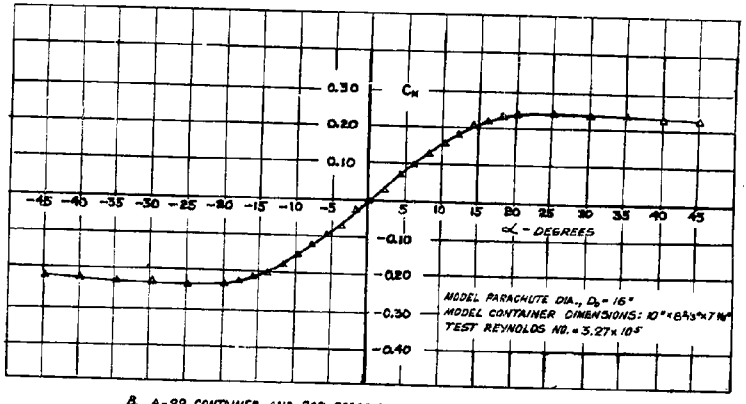

B. A-22 CONTAINER AND 20% POROSITY 96" DIA. RIBBON PARACHUTE

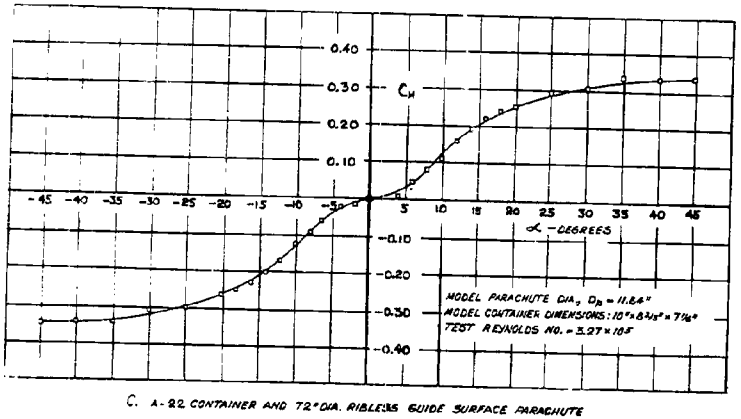

C. A-22 CONTAINER AND 72" DIA. RIBLESS GUIDE SURFACE PARACHUTE

FIG. 23 - MOMENT COEFFICIENT FOR MODEL SYSTEMS REPRESENTING THE A-22 CONTAINER WITH THREE PARACHUTE TYPES WITH NO RISERS

an angle of attack of ± 25 degrees. For this configuration, $(dC_m/d\alpha)_{\alpha=0}$ was less than the value for the ring slot combination.

The moment coefficients for the container with the 72 inch diameter ribless guide surface parachute are presented in Fig 23-C. This plot reveals that the configuration is stable for all angles in the region tested. This combination has the smallest $(dC_m/d\alpha)_{\alpha=0}$ of the three configurations tested.

Figure 24 presents, for comparison purposes, the moment coefficient versus α for the ring slot, ribbon, and ribless guide surface parachute container configurations given above when used with no risers.

3.5.1.3 Tests with Parachute Models Representing Solid Flat, Ribbon, and Ring Slot Parachutes of 64 inch Diameter and a Ribless Guide Surface Parachute of 48 inch diameter

Figure 25-A shows the moment characteristics for a system with a 64 inch diameter solid flat parachute attached to the A-22 Container with no risers. It indicates a stable configuration over the range tested (± 35 degrees). The maximum stable moment coefficient was $C_M = 0.145$ at 18.5 degrees. In addition, this combination appeared to have the largest value of $(dC_m/d\alpha)_{\alpha=0}$.

Figure 25-B indicates that a 20% porosity 64 inch diameter ring slot parachute attached to the container with no risers gives a stable configuration over the range tested (± 30 degrees). This combination has a maximum stable moment coefficient $C_M = 0.082$ at 15 degrees, and the slope of the

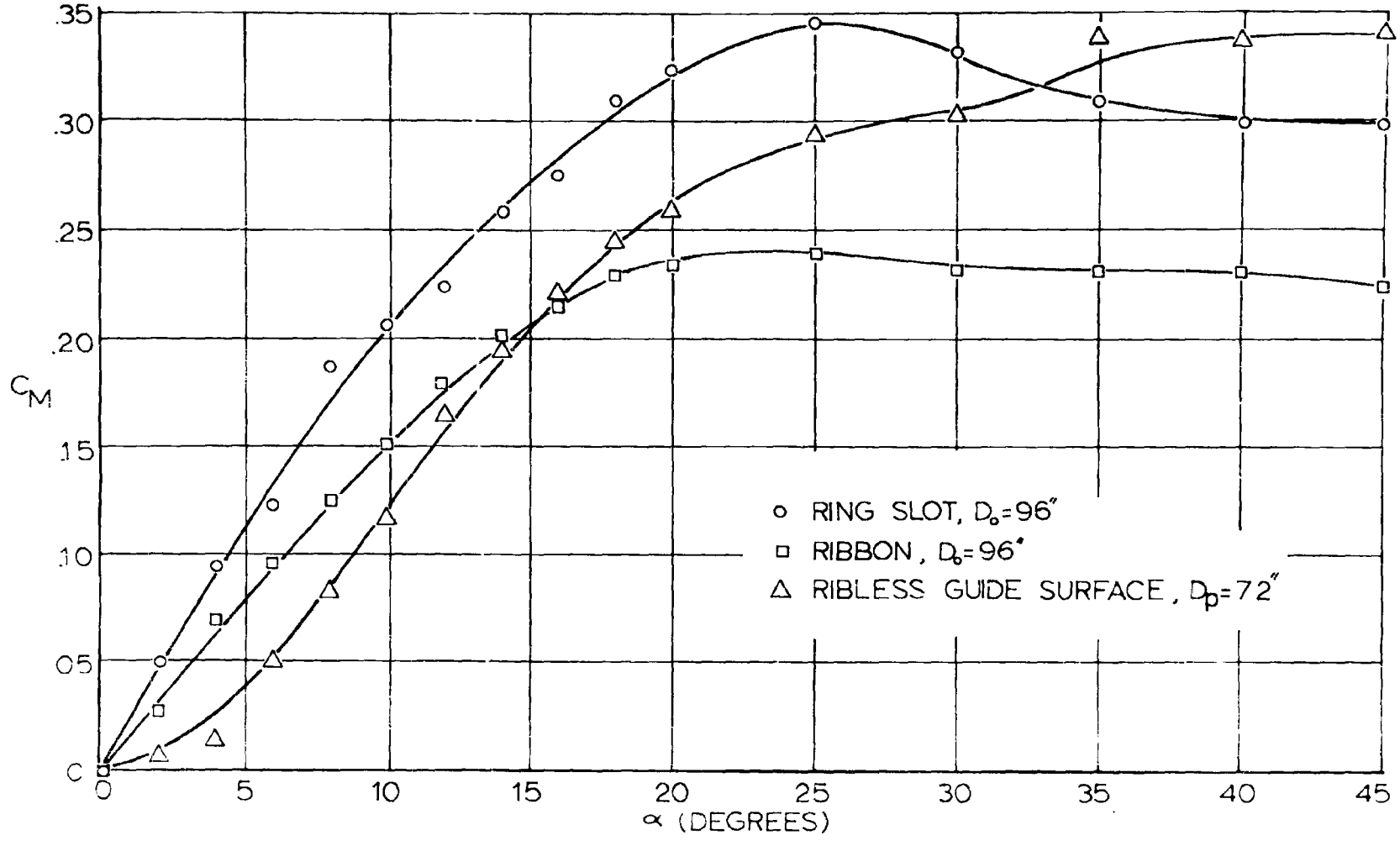

FIG. 24 - MOMENT COEFFICIENT FOR A-22 CONTAINER AND VARIOUS PARACHUTE MODELS WITH NO RISERS

TEST REYNOLDS NO. = 3.66×10^5 CONTAINER DIMENSIONS 10" x $8\frac{2}{3}$" x $7\frac{1}{2}$"

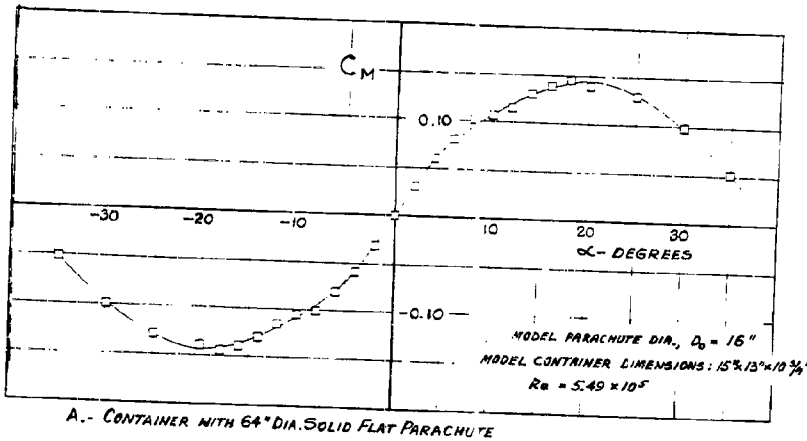

A.- CONTAINER WITH 64" DIA. SOLID FLAT PARACHUTE

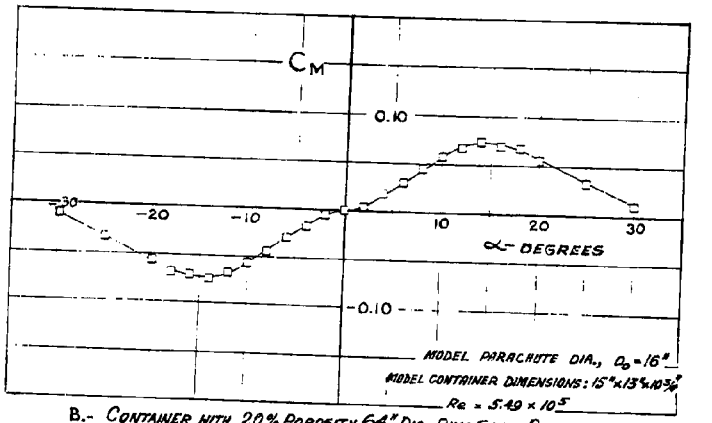

B.- CONTAINER WITH 20% POROSITY 64" DIA. RING SLOT PARACHUTE

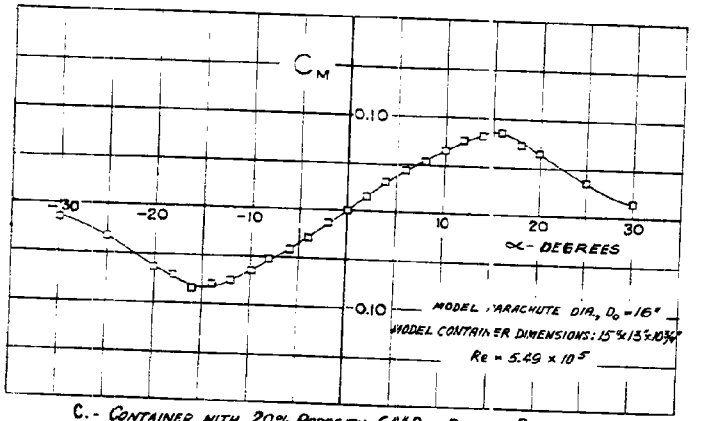

C.- CONTAINER WITH 20% POROSITY 64" DIA. RIBBON PARACHUTE

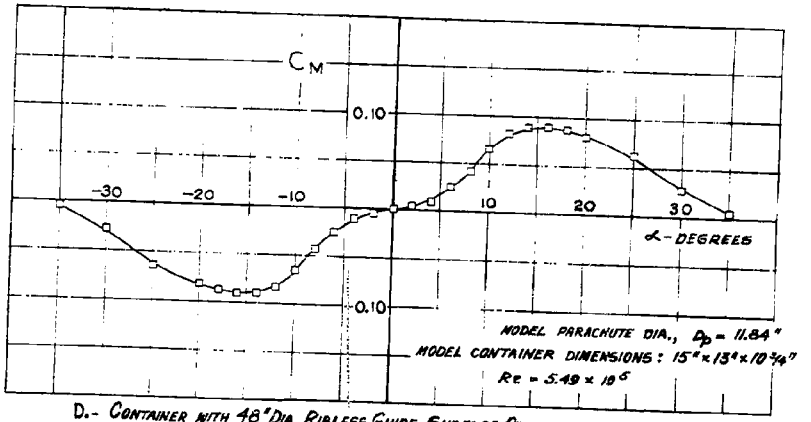

D.- CONTAINER WITH 48" DIA. RIBLESS GUIDE SURFACE PARACHUTE

FIG. 25 - MOMENT COEFFICIENT FOR MODEL SYSTEMS REPRESENTING THE A-22 CONTAINER WITH FOUR PARACHUTE TYPES WITH NO RISERS

moment coefficient curve at zero angle of attack is larger than for either the guide surface or ribbon combinations.

Figure 25-C shows the moment coefficient versus the angle of attack for the 20% porosity 64 inch diameter ribbon parachute container configuration with no risers. This configuration is stable over the range $\alpha = \pm 32$ degrees, and the maximum stable moment coefficient measured was 0.074 at $\alpha = 14$ degrees. The value $(dC_m/d\alpha)_{\alpha = 0}$ is very small.

Figure 25-D indicates that a 48 inch diameter ribless guide surface parachute attached to the container with no risers produces a stable configuration over the range $\alpha = \pm 36$ degrees. The maximum stable moment coefficient measured was 0.09 at $\alpha = 16$ degrees. The slope of the moment coefficient curve at zero angle of attack $(dC_m/d\alpha)_{\alpha = 0}$ is very small.

Figure 26 presents, for comparison purposes, the moment coefficient versus α for each of the four parachute container combinations listed above with no risers.

3.5.2 Drag Characteristics

The experimental values of the drag coefficients for the container alone and the system drag when the container is set at $\alpha = 0$ for each of the three scale models in conjunction with the four parachute types without risers are given in Fig 27 and illustrated in Fig 28. The drag forces were measured by means of the strain gage drag balance incorporated in the vertically mounted container pivotal shaft and described in Paragraph 2.6. Drag measurements were not originally envisaged but were deemed very desirable for comparison of the relative merits of

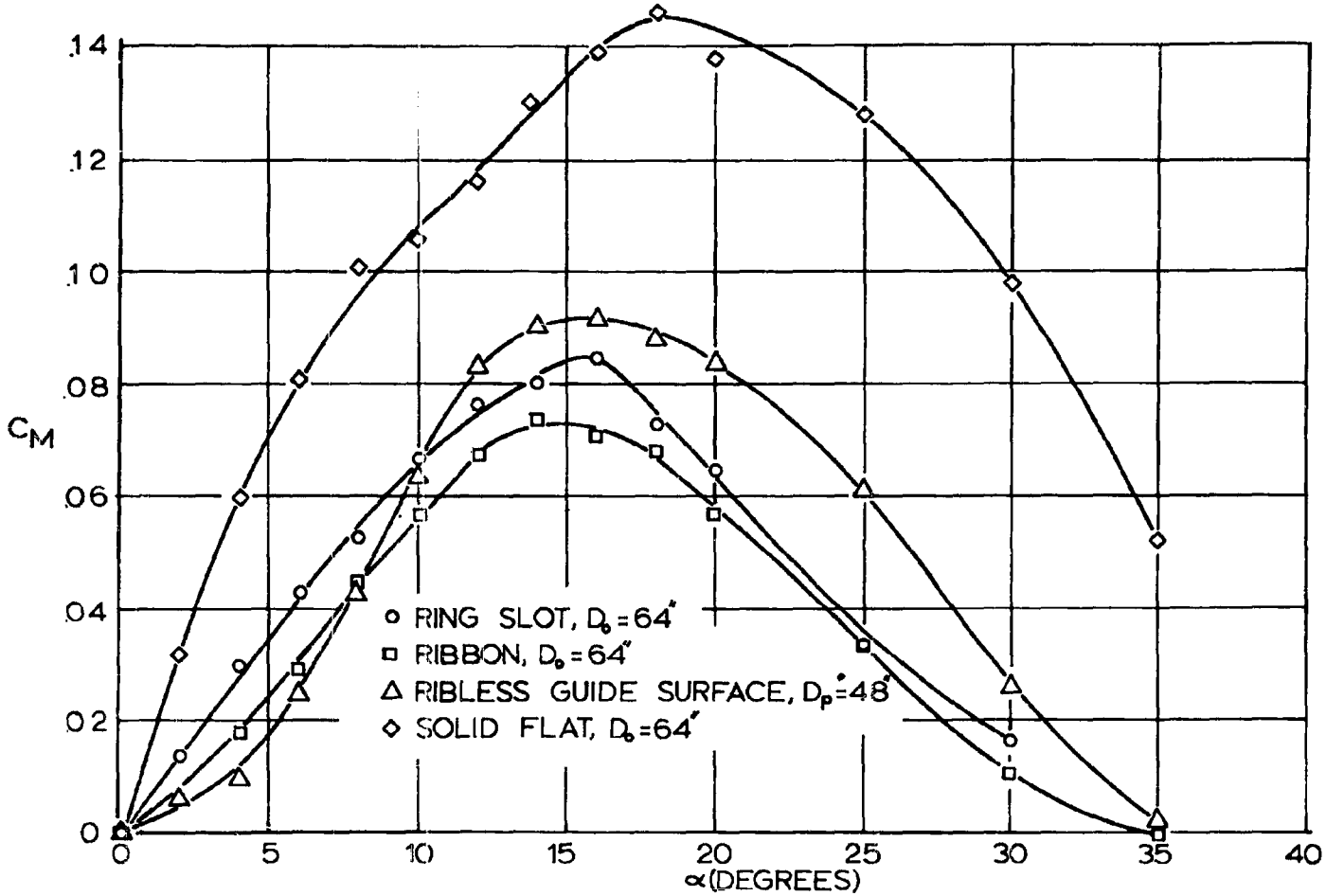

FIG. 26- MOMENT COEFFICIENT FOR A-22 CONTAINER AND VARIOUS PARACHUTE MODELS WITH NO RISERS

TEST REYNOLDS NO. = 5.49×10^5 CONTAINER DIMENSIONS: $15" \times 13" \times 10\frac{3}{4}"$

		AVERAGE DRAG COEFFICIENT AND FULL SCALE PARACHUTE DIAMETER		
		1/8 SCALE	1/6 SCALE	1/4 SCALE
CONTAINER ALONE	C_D	0.802	0.950	0.804
CONTAINER AND SOLID FLAT PARACHUTE	C_D	5.509	- - -	1.507
	D_o	128 IN.	- - -	64 IN.
CONTAINER AND RING SLOT PARACHUTE	C_D	3.930	2.660	1.170
	D_o	128 IN.	96 IN.	64 IN.
CONTAINER AND RIBLESS GUIDE SURFACE PARACHUTE	C_D	3.690	2.550	1.230
	D_p	96 IN.	72 IN.	48 IN.
CONTAINER AND RIBBON PARACHUTE	C_D	3.530	2.380	1.160
	D_o	128 IN.	96 IN.	64 IN.

FIG. 27- AVERAGE DRAG COEFFICIENTS BASED ON CONTAINER BASE AREA FOR VARIOUS SCALE CONTAINER-PARACHUTE COMBINATIONS WITH NO RISERS

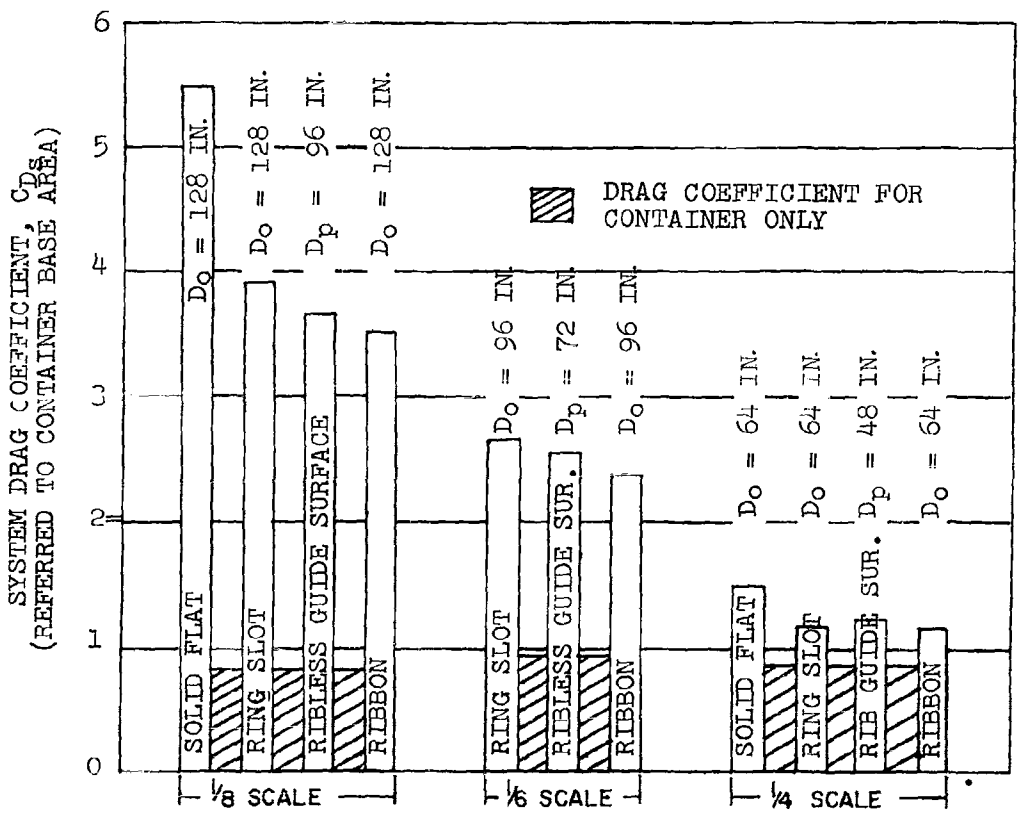

FIG. 28- DRAG COEFFICIENTS FOR VARIOUS CONTAINER-PARACHUTE COMBINATIONS. CONTAINER BASE REFERENCE AREA: 15.53 FT^2

the different parachutes and the selection of an optimum type.

The drag coefficients presented in Fig 28 are all calculated with the container base area, namely 15.53 ft^2 full scale, as reference, and this explains the reason why the numerical values are very large, particularly for the cases representing the largest parachute namely, 128 in. for the solid flat, ribbon and ring slot parachutes and 96 in. for the ribless guide surface type. Figure 28 shows that, for the cases of the smallest parachutes represented, namely 64 in. for the solid flat, ribbon and ring slot and 48 in. for the ribless guide surface, the additional drag due to the parachutes is but a small fraction of the drag of the container alone. This drag represents a 44% increase for the ribbon parachute case, a 46% increase for the ring slot parachute, a 53% increase for the ribless guide surface parachute, and an 87% increase for the solid flat parachute.

It is significant that the total drag coefficient with the ribless guide surface parachute is higher than that with the ribbon parachute for all container scales.

3.5.3 Parachute and Container Free Attitude Angles

After recording the moment and drag characteristics, the locking arrangement on the pivotal shaft was released, the container angular measuring device and the parachute attitude measuring device were activated, and the free angles α, θ, and ψ for the four types of parachutes in conjunction with different scale containers were recorded These tests were made with no risers between the container spider web and the

parachute suspension lines. Figures 29-A, B, and C are photographs of the experimental arrangement of the 1/4 scale container in combination with parachutes representing full scale diameters of 64 in. for the ringlsot and ribbon types and 48 in. for the ribless guide surface parachute with no risers.

From a visual observation of the behavior of the freely suspended container and parachute models for different parachute types and container scales, the following qualitative remarks can be made.

The solid flat parachute (Fig 30-A) exhibited very large amplitude random motion and violent oscillations for all container scales. This parachute appeared to be the least suitable for stabilization of the A-22 Container. The ring slot parachute model (Fig 30-B) exhibited some oscillation of the parachute about the container's longitudinal axis for the different configurations but was decidedly more suitable than the solid flat type. The oscillations of the container about its pivotal axis and the random motions of the parachute axis appeared to be much smaller for the ribbon parachute model in its various configurations (Fig 30-C). The various configurations using the ribless guide surface parachute model appeared to exhibit the smallest departures in container axis angle α and parachute mean attitude angles θ and ψ from the axial flow direction, although the frequency of oscillation of the container and parachute model was higher than that of the other types (Fig 30-D). Both the ribbon and the ribless guide surface parachutes appeared to be quite satisfactory for stabilizing the A-22 Container.

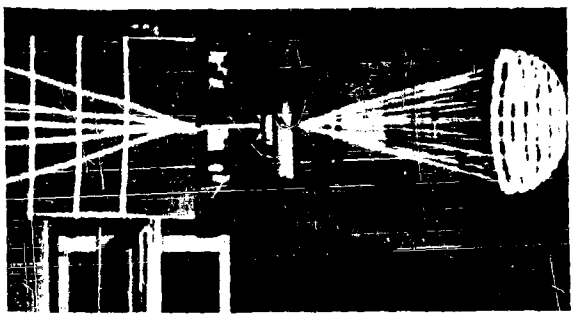

A. MODEL ARRANGEMENT REPRESENTING CONTAINER AND 20% POROSITY 64" DIA. RING SLOT PARACHUTE

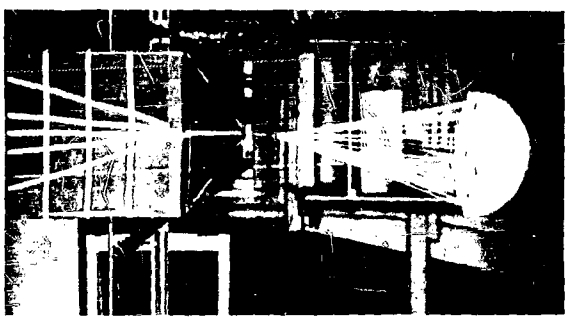

B. MODEL ARRANGEMENT REPRESENTING CONTAINER AND 20% POROSITY 64" DIA. RIBBON PARACHUTE

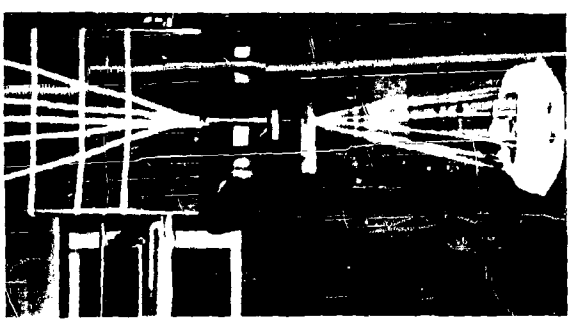

C. MODEL ARRANGEMENT REPRESENTING CONTAINER AND 48" DIA. RIBLESS GUIDE SURFACE PARACHUTE

FIG. 29-EXPERIMENTAL ARRANGEMENT OF THE 1/4 SCALE A-22 CONTAINER IN COMBINATION WITH THREE PARACHUTE TYPES WITH NO RISERS

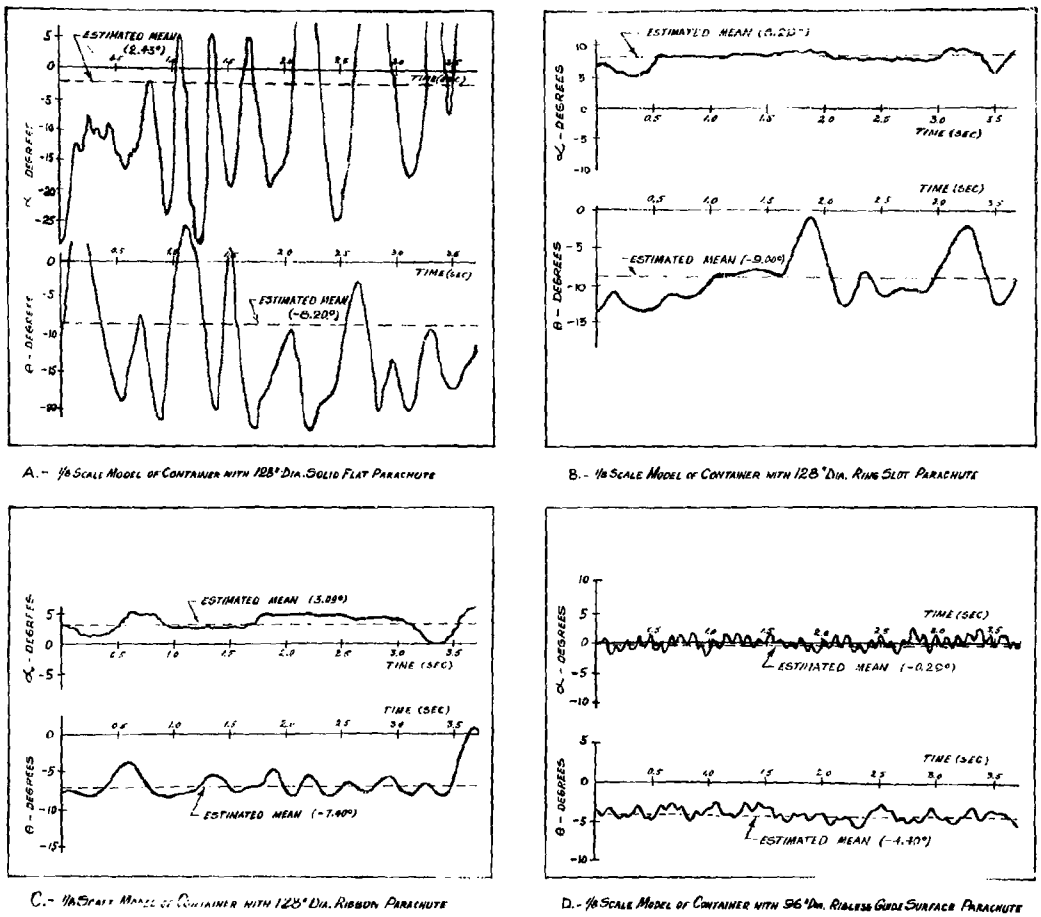

A.- 1/8 Scale Model of Container with 128" Dia. Solid Flat Parachute

B.- 1/8 Scale Model of Container with 128" Dia. Ring Slot Parachute

C.- 1/8 Scale Model of Container with 128" Dia. Ribbon Parachute

D.- 1/8 Scale Model of Container with 96" Dia. Ribless Guide Surface Parachute

FIG. 30 - COMPARATIVE STABILITY BEHAVIOR OF THE A-22 CONTAINER WITH VARIOUS TYPES OF PARACHUTES AND NO RISERS CONTAINER AND PARACHUTE ATTITUDE ANGLES α AND θ VERSUS TIME. $Re = 2.75 \times 10^5$

In our experimental arrangement, the parachute models are suspended horizontally behind the container model in the test section and the weight of the parachute tends to produce a positive attitude angle ψ which depends on the parachute model weight, the aerodynamic forces involved, and the riser length. For this reason, the angle ψ as measured is not representative of actual aerial delivery conditions where the path is more nearly vertical for most of the trajectory after full deployment. Therefore, the recorded angles ψ are not illustrated.

3.6 Tests with Parachute Stabilized Container Models with Risers

Since risers are invariably used in aerial delivery, a series of tests with scaled down riser lengths corresponding to 10, 20, and 30 ft were carried out. These tests included recording the moment characteristics, the system drag at zero container angle of attack, and the free attitude angles. They involved parachute container configurations representing full scale parachute diameters of 96 in. and 64 in. for the ribbon and ring slot parachutes and 72 in. and 48 in. for the ribless guide surface type.

3.6.1 Moment Characteristics

3.6.1.1 Tests representing 96 in. Ribbon and Ring Slot Parachutes and a 72 in. Ribless Guide Surface Parachute

In practically all tests with risers, the full angular range of $\pm$ 90 degrees was used and the values obtained for the

moment coefficients at identical positive and negative angles of attack were averaged to account for minor flow variations in the test section. To limit the number of experimental tests and data points to a reasonable amount, we conducted no moment tests with risers with the solid flat parachute container combination. Tests without risers had established the relative inferiority of this type of parachute in comparison with the other three types.

Figures 31-A, B, and C illustrate the variation of the moment coefficients with the container angle of attack for the 96 in. diameter ring slot and ribbon and the 72 in. diameter ribless guide surface parachute container configurations without risers and with risers representing 10, 20, and 30 ft length in full scale.

It is apparent that the use of risers considerably increases the stabilizing moment coefficient particularly at large container angles.

It is also significant that, except for the ribbon parachute at large angles α, relatively little changes of C_m occur for increased riser lengths beyond 10 ft suggesting that other things being equal, a 10 ft riser would be adequate for this configuration.

Figures 32-A, B, and C present, for comparison purposes, the moment coefficients for the 96 in. ring slot and ribbon and the 72 in. ribless guide surface parachute when used with risers representing 10, 20, and 30 ft full scale respectively. Figure 32-A shows that for a 10 ft riser length, the ring slot

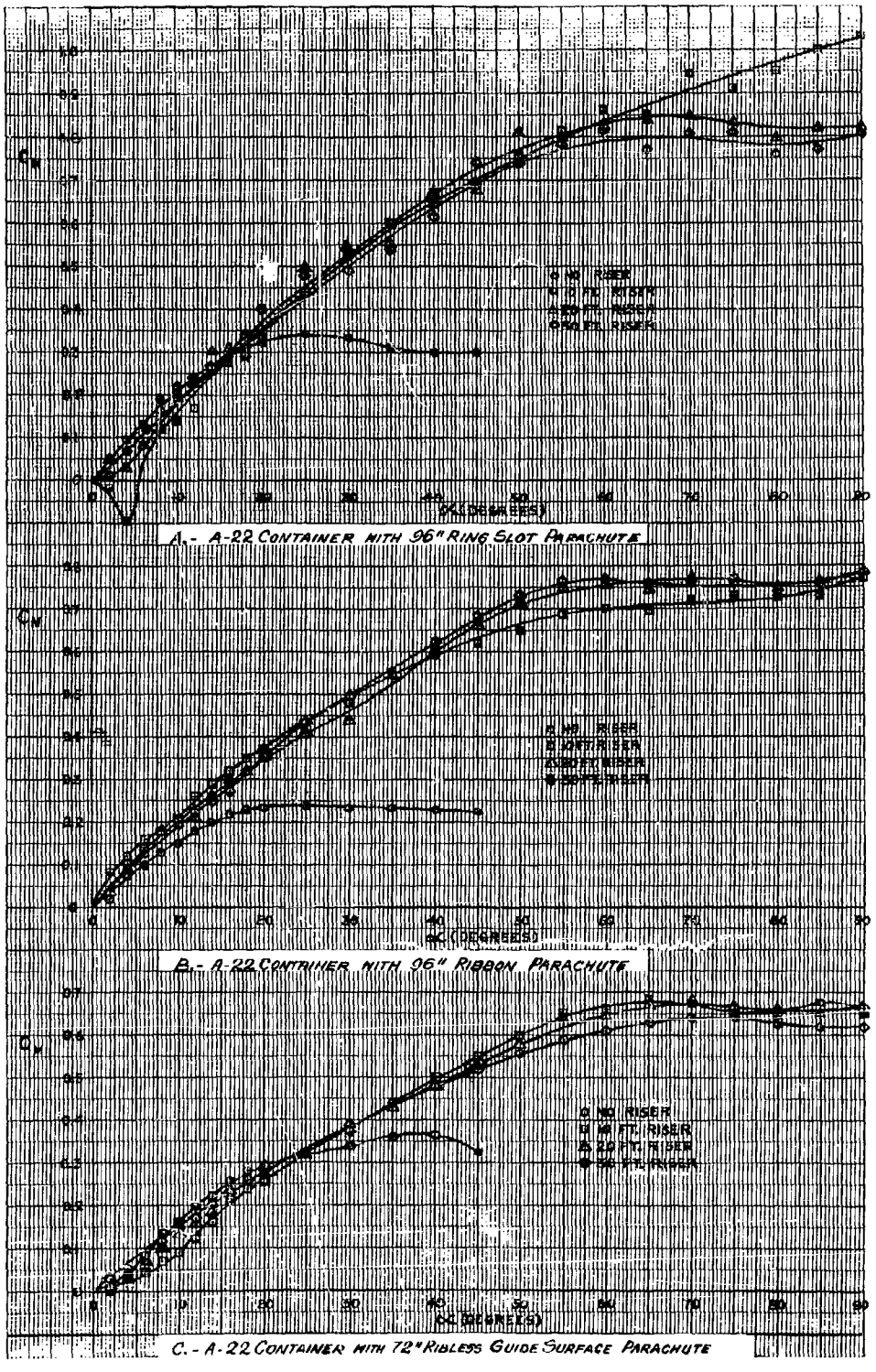

FIG. 31 - MOMENT COEFFICIENT FOR MODELS REPRESENTING VARIOUS RISER LENGTHS AND PARACHUTE-CONTAINER COMBINATIONS. $Re = 3.66 \times 10^5$, $q = 5.20$ LB/SQ. FT.

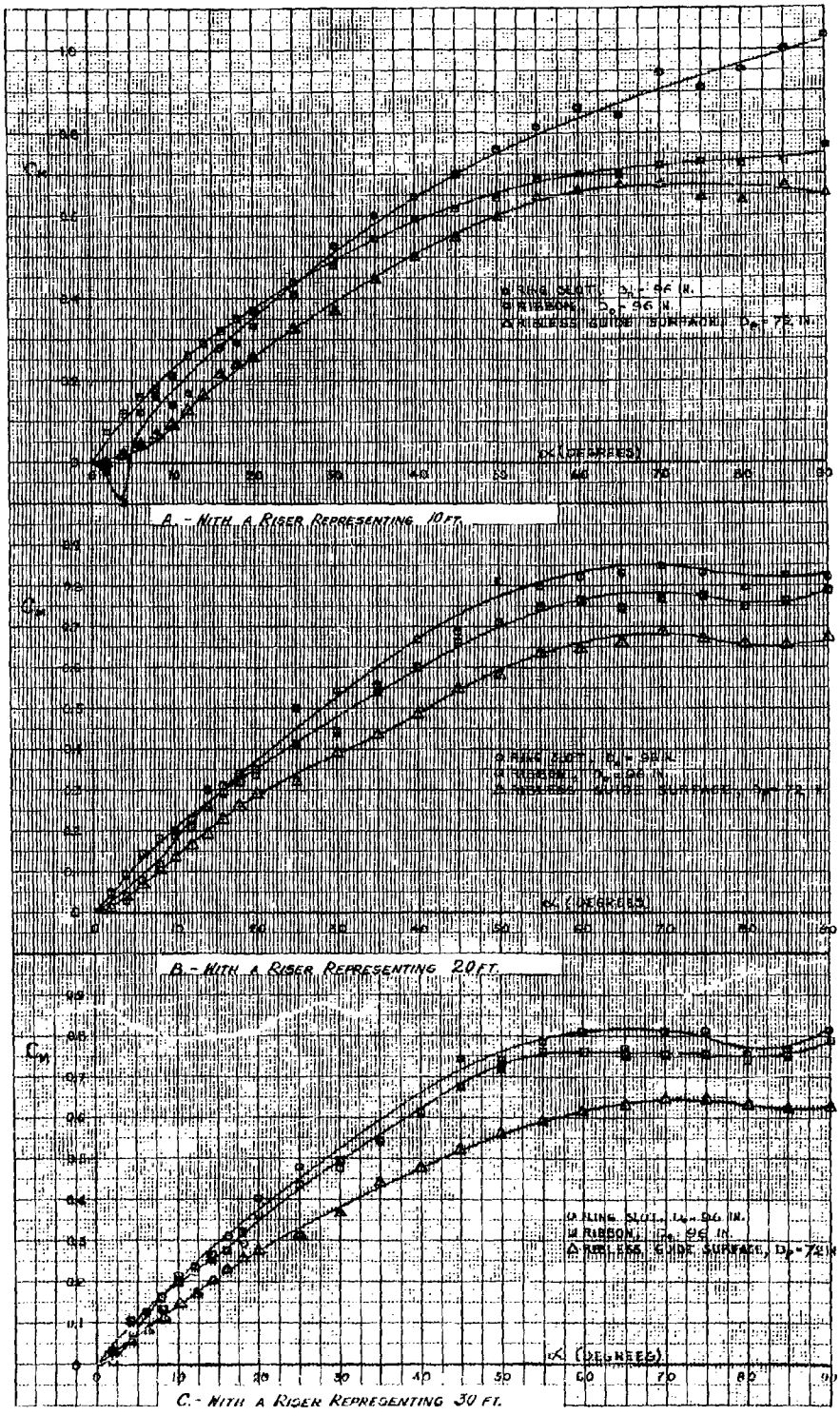

FIG. 32 - MOMENT COEFFICIENT FOR VARIOUS PARACHUTE-CONTAINER COMBINATIONS AND RISER LENGTHS. $R_e = 3.66 \times 10^4$; $q = 5.10$ lbs/sq ft

parachute configuration has a small unstable range of $\pm$ 5 degrees and the largest stabilizing moment coefficients at large angles of attack.

The ribbon parachute configuration has the largest moment coefficient slope at zero angle of attack $(dC_m/d\alpha)_{\alpha = 0}$ of the three types tested, while the ribless guide surface has a very small value of $(dC_m/d\alpha)_{\alpha = 0}$ and a smaller value of the moment coefficient over practically the full angular range.

Figure 32-B indicates that for a 20 ft riser length the ring slot and ribbon parachute configurations have nearly the same moment coefficients over the full angular range while the ribless guide surface container combination has smaller C_m values over practically the entire angular range.

Similar conclusions can be drawn from Fig 32-C for a 30 ft full scale riser length.

3.6.1.2 Tests Representing 64 in. Ribbon and Ring Slot Parachutes and a 48 in. Ribless Guide Surface Parachute

Figures 33-A, B, and C show the variation of the moment coefficients with the container angle of attack for the 64 in. ring slot and ribbon parachutes and the 48 in. ribless guide surface parachute configurations without risers and with risers representing 10, 20, and 30 ft lengths in full scale.

It is apparent from Figs 33-A, B, and C that the use of risers considerably improves the stabilizing characteristics and produces a stable configuration over the full angular range of $\pm$ 90 degrees instead of a limited angular range of about $\pm$ 35 degrees for the cases without risers.

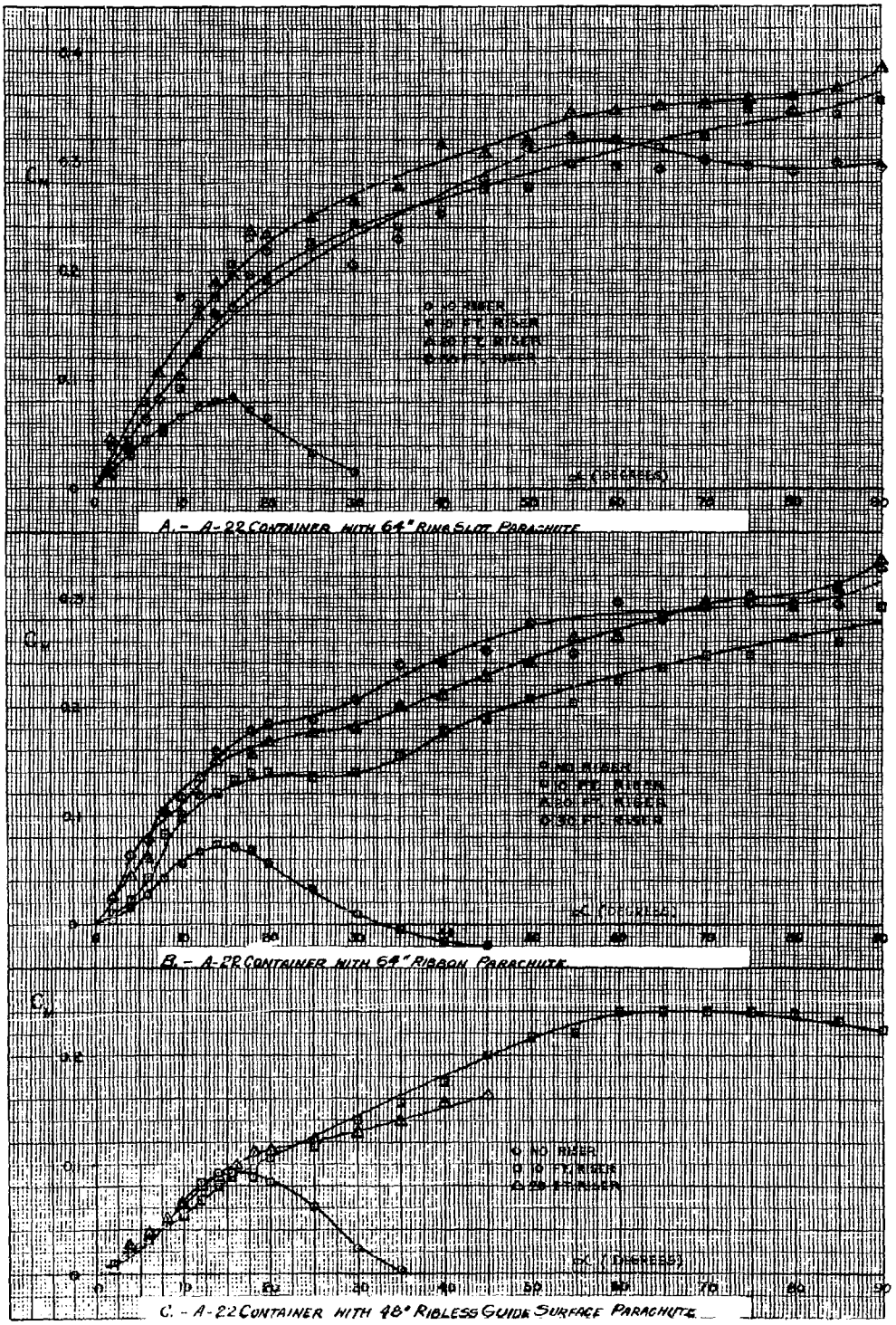

FIG. 33 - MOMENT COEFFICIENT FOR MODELS REPRESENTING VARIOUS RISER LENGTHS AND PARACHUTE - CONTAINER COMBINATIONS
$R_E = 5.49 \times 10^5$; $q = 5.20$ LB/SQ. FT.

For the 64 in. ring slot container configuration, Fig 33-A indicates that a 20 ft riser produces larger stabilizing moment coefficients over the full angular range than either the 10 ft or 30 ft risers.

Figure 33-B shows that the 64 in. ribbon parachute container combination without risers is unstable beyond $\alpha = 33$ degrees. The use of risers stabilizes this configuration over the full angular range. The 20 and 30 ft risers produce substantially the same stable moment coefficients over a large part of the angular range and these coefficients are appreciably larger than those with a 10 ft riser.

Figure 33-C shows that the 48 in. ribless guide surface parachute container combination is unstable beyond $\alpha = 35.5$ degrees. The use of risers, however, produces stable moment coefficients over the full angular range. For this configuration, it was not possible to test with the 30 ft riser or to carry the 20 ft riser case beyond 45 degrees. This was due to the particular character of the flow in the open test section which produced a secondary flow that carried the very light parachute model outside the test section. This condition is peculiar to the testing arrangement and would not be reflected in full scale, free flight.

Figures 34-A, B, and C present, for comparison purposes, the moment coefficients for the 64 in. ring slot and ribbon and the 48 in. ribless guide surface parachute models when used in conjunction with the A-22 container with risers representing 10, 20, and 30 ft full scale respectively.

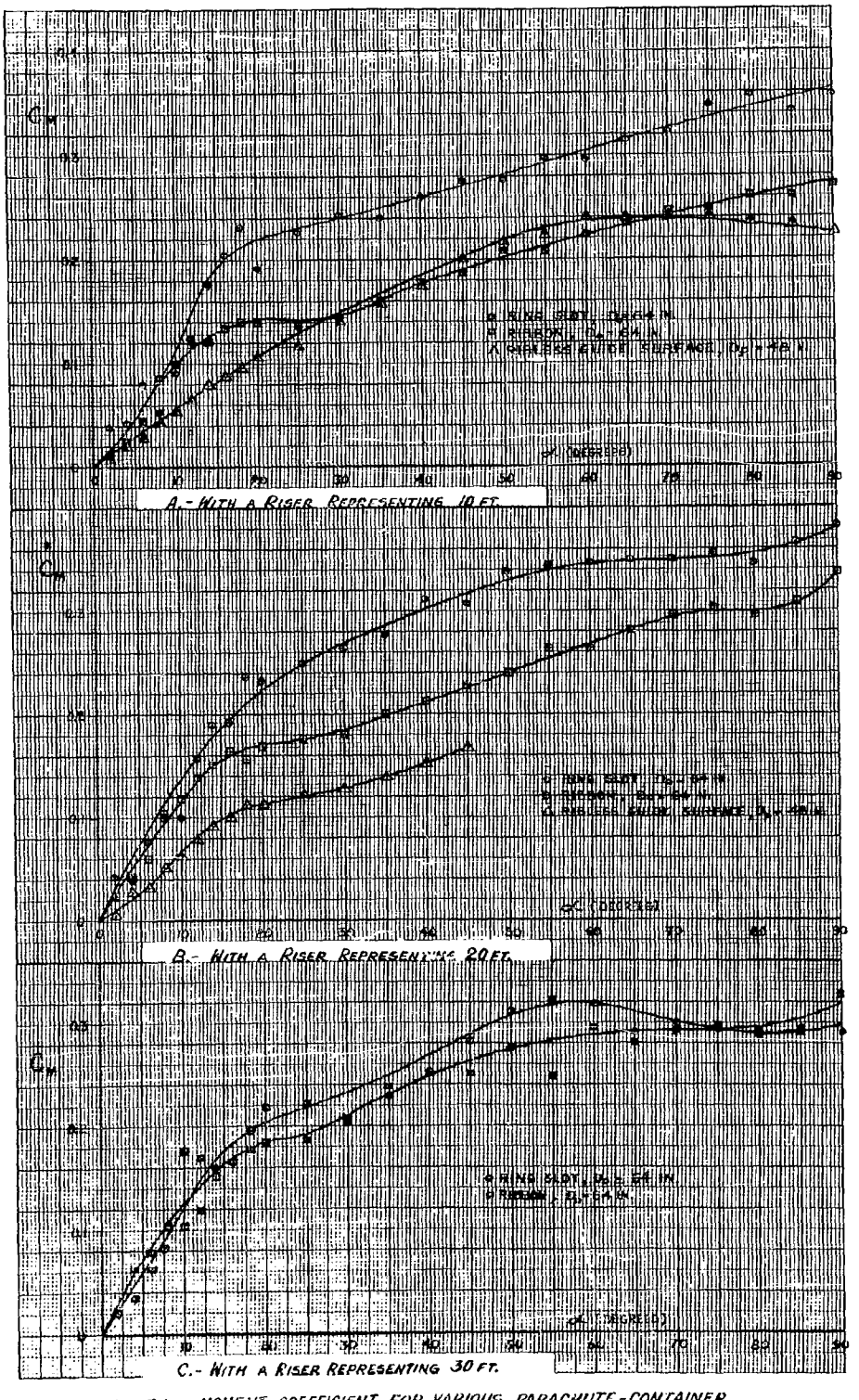

FIG. 34 - MOMENT COEFFICIENT FOR VARIOUS PARACHUTE-CONTAINER COMBINATIONS AND RISER LENGTHS. $Re = 5.49 \times 10^5$; $q = 5.20$ LB/SQ. FT.

Figure 34-A shows that, for the 10 ft riser case, the 64 in. ribbon and the 48 in. ribless guide surface parachute configurations have substantially the same moment coefficients over most of the range while the 64 in. ring slot configuration has considerably larger moment coefficients over the full angular range.

For the 20 ft riser case, Fig 34-B indicates the stable moment coefficients to be largest for the 64 in. ring slot parachute, smallest for the 48 in. ribless guide surface parachute, and intermediate for the 64 in. ribbon parachute.

3.6.2 Drag Characteristics

3.6.2.1 Tests Representing 96 in. Ribbon and Ring Slot Parachutes and 72 in. Ribless Guide Surface Parachutes

Figures 35-A, B, and C present the individual drag coefficients of the container and the parachute as well as the drag coefficients of the combination or system drag for the A-22 Container with the 96 in. ring slot and ribbon and the 72 in. ribless guide surface parachutes for riser lengths of 10, 20, and 30 ft. In all cases, the drag coefficients are based on the container base area and this explains why the drag coefficients of the container alone and the parachute alone are also plotted for comparison with the system drag.

The drag coefficients of the parachutes alone steadily decrease with increasing riser length. This is mainly due to the fact that the flow downstream of the contraction in the free jet is not uniform and there exists a velocity gradient in the longitudinal direction. However, the differences are quite

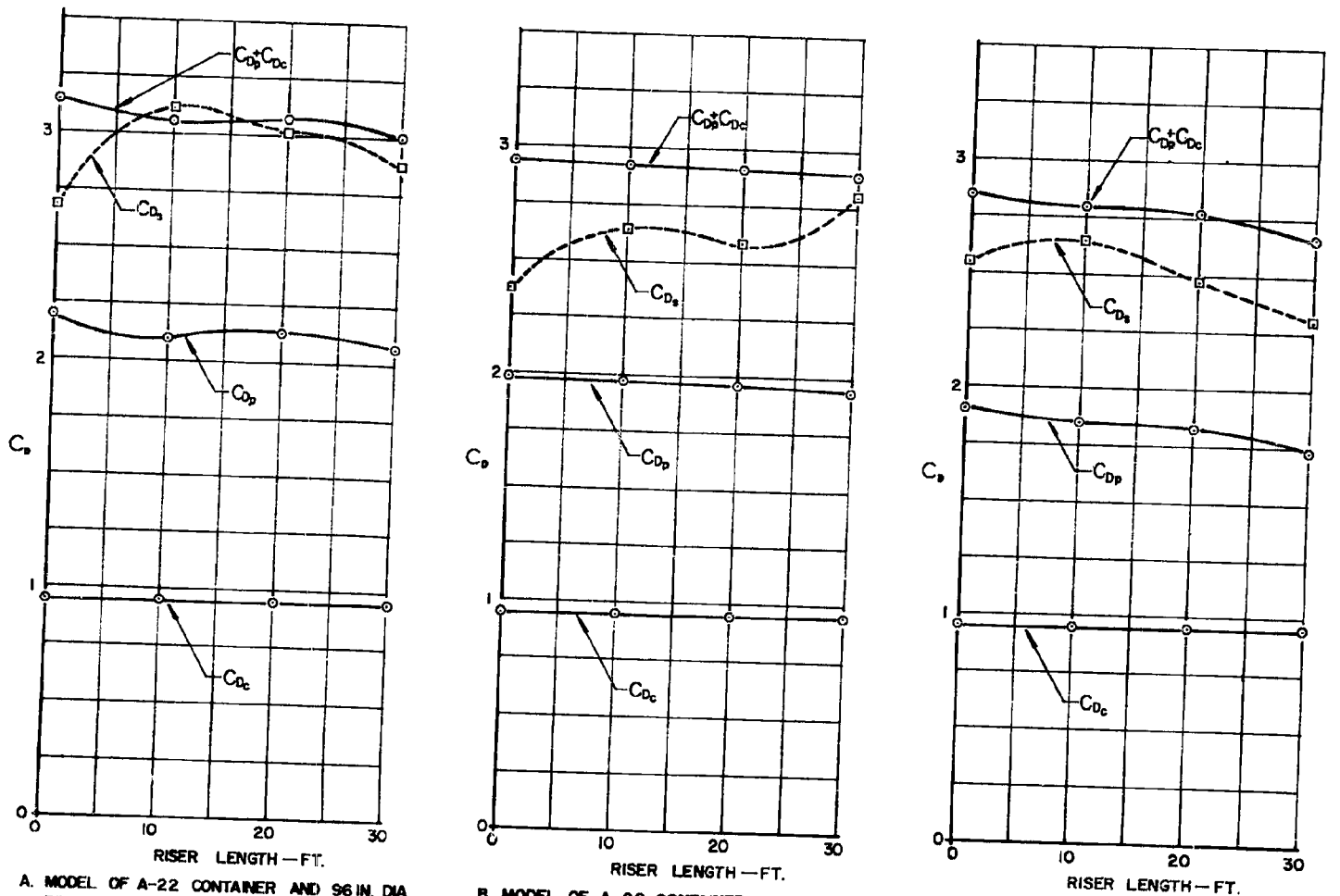

A. MODEL OF A-22 CONTAINER AND 96 IN. DIA RING SLOT PARACHUTE

B. MODEL OF A-22 CONTAINER AND 96 IN. DIA RIBBON PARACHUTE

C. MODEL OF A-22 CONTAINER AND 72 IN. DIA RIBLESS GUIDE SURFACE PARACHUTE

FIG. 35- DRAG COEFFICIENT VERSUS RISER LENGTH FOR VARIOUS PARACHUTE-CONTAINER COMBINATIONS

$Re = 3.66 \times 10^5$; $q = 5.20$ LB/FT^2

small, particularily for riser lengths representing 20 ft or less.

Figure 35-A shows that, for the 96 in. ring slot parachute container configuration, the system drag coefficient is increased by about 15% by using a 10 ft riser. For this case, the system drag coefficient is substantially equal to the sum of the drag coefficients of the container and parachute models taken separately. There is a very slight reduction of system drag coefficient for the 20 ft riser and an appreciable reduction for the 30 ft riser case. This appears to be largely due to the longitudinal velocity gradient.

Figure 35-B for the 96 in. ribbon parachute container configuration indicates that the system drag coefficient is maximum for the 30 ft riser but the absolute values are somewhat smaller than the ring slot case, and the system drag is, for all riser lengths, smaller than the sum of the drag of the individual container and parachute.

Figure 35-C for the 72 in. ribless guide surface parachute container configuration shows that the use of a 10 ft riser produces only a small increase of system drag (about 4%). For risers of 20 and 30 ft, the system drag coefficients decrease far more than would be expected from the decrease of drag coefficient of the parachute alone. The reason for this effect could not be ascertained.

Figure 36 shows, for comparison, the system drag coefficient for the A-22 Container stabilized by the 96 in. ring slot and ribbon parachutes and the 72 in. ribless guide surface parachute using risers of 0, 10, 20, and 30 ft.

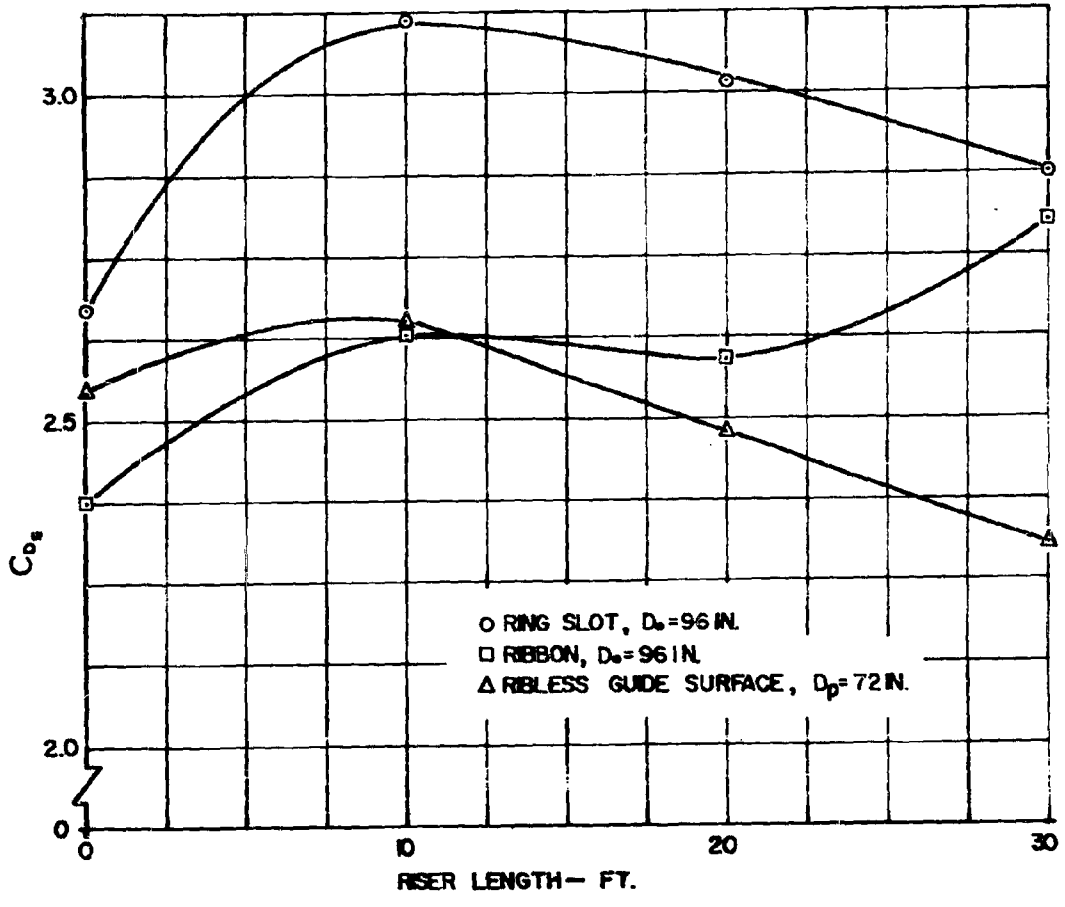

FIG. 36- SYSTEM DRAG COEFFICIENT VERSUS RISER LENGTH FOR DIFFERENT PARACHUTE CONTAINER COMBINATIONS

$Re = 3.66 \times 10^5$; $q = 5.20$ LB./FT^2

It is apparent that, for the same riser length, the system drag is appreciably larger for the configuration employing the ring slot parachute, while the ribbon and ribless guide surface parachutes produce substantially the same drag for riser lengths of 0, 10, and 20 ft. For a riser of 30 ft, however, the ribbon parachute produces an appreciably larger system drag coefficient $C_{D_S} = 2.81$ compared to $C_{D_S} = 2.31$ for the ribbon guide surface case.

3.6.2.2 Tests Representing 64 in. Ribbon and Ring Slot Parachutes and 48 in. Ribless Guide Surface Parachute

Figures 37-A, B, and C present the individual drag coefficients of the container and the parachute as well as the system drag coefficients for the container with the 64 in. ring slot and ribbon parachutes and the 48 in. ribless guide surface parachute for riser lengths of 0, 10, 20, and 30 ft full scale. The summation of the individual drag coefficients of the container and parachute is also plotted in these figures for comparison with the system drag.

Figure 37-A shows that for the 64 in. ring slot parachute container configuration, the use of a riser produces a considerable increase of drag coefficient. With no risers, the system drag coefficient is 1.17; with a 10 ft riser, the drag coefficient is increased to 1.89 and reaches a maximum value of 2.05 for a 20 ft riser and then is reduced to 1.80 for a 30 ft riser. It is significant that for this configuration, the system drag coefficient is larger than the sum of the individual drag coefficients for all cases using risers.

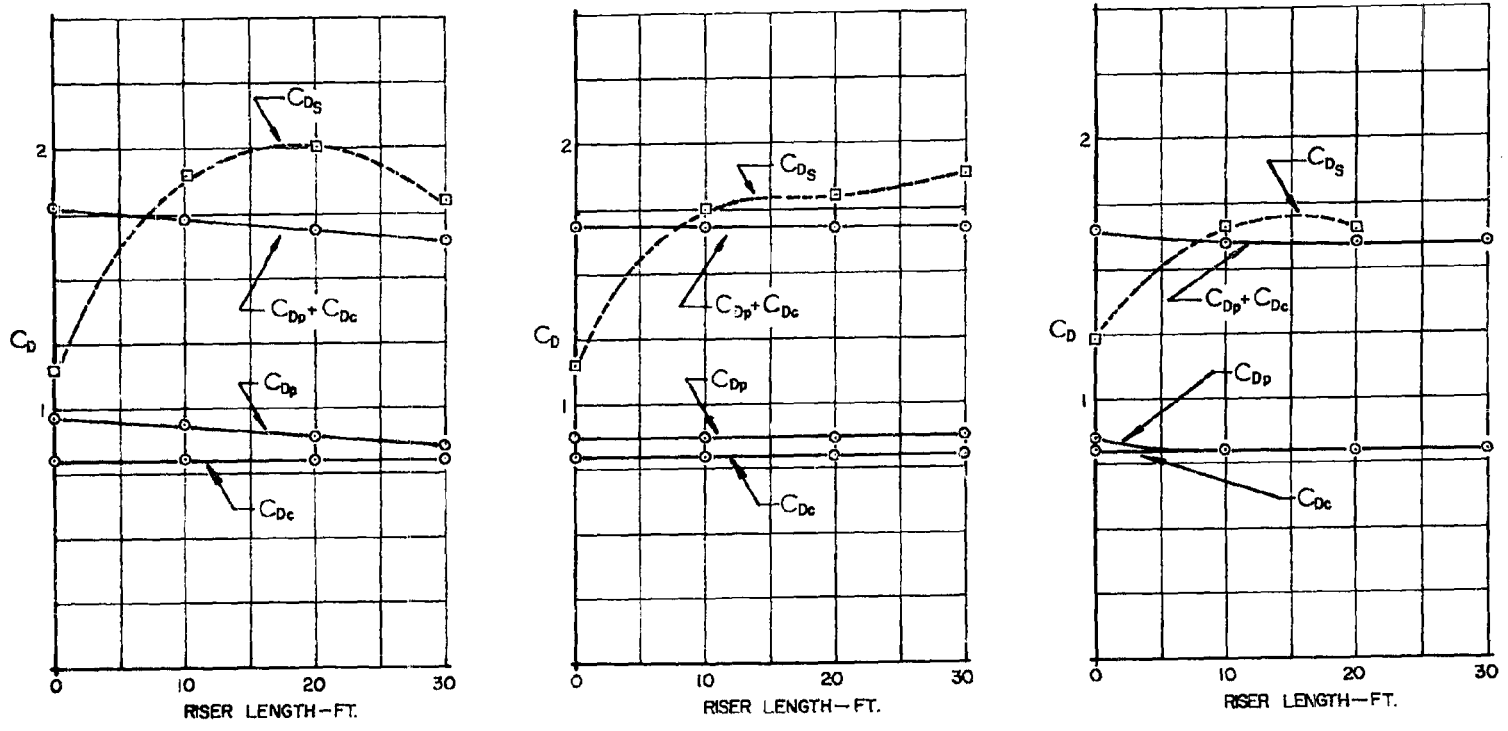

A.—MODEL OF A-22 CONTAINER AND 64" DIA. RING SLOT PARACHUTE

B.—MODEL OF A-22 CONTAINER AND 64" DIA. RIBBON PARACHUTE

C.—MODEL OF A-22 CONTAINER AND 48" DIA. RIBLESS GUIDE SURFACE PARACHUTE

FIG. 37- DRAG COEFFICIENT VERSUS RISER LENGTH FOR VARIOUS PARACHUTE-CONTAINER COMBINATIONS.

$Re = 5.49 \times 10^5$, $q = 5.20$ LB/FT^2

Figure 37-B for the 64 in. ribbon parachute container configuration shows that the system drag coefficient without risers C_{D_s} = 1.16; this increases to C_{D_s} = 1.77 for a 10 ft riser, C_{D_s} = 1.80 for a 20 ft riser, and C_{D_s} = 1.87 for a 30 ft riser. Again, it is noted that the system drag coefficient C_{D_s} is larger than the sum of the individual drag coefficients $C_{D_p} + C_{D_c}$ for all cases using risers.

Figure 37-C for the 48 in. ribless guide surface parachute container configuration shows a system drag coefficient C_{D_s} = 1.23 without risers, increasing to 1.65 for a 10 ft and a 20 ft riser. For this configuration, the system drag coefficient is again found to be larger than the sum of the individual drag coefficients although the difference is much smaller than the ribbon or ring slot configurations.

It would appear from Figs 37-A, B, and C that with the relatively large container and correspondingly large wake, a positive "interference effect" takes place resulting in greater system drag coefficient than the sum of the individual drag coefficients. This is not the case for the previous tests where the interference effect was negative, i.e., producing a system drag coefficient smaller than the sum of the individual drag coefficients.

Figure 38 shows, for comparison, the system drag coefficient for the A-22 Container stabilized by the 64 in. ring slot and ribbon parachutes, and the 48 in. ribless guide surface parachute using risers of 0, 10, 20, and 30 ft. It is apparent

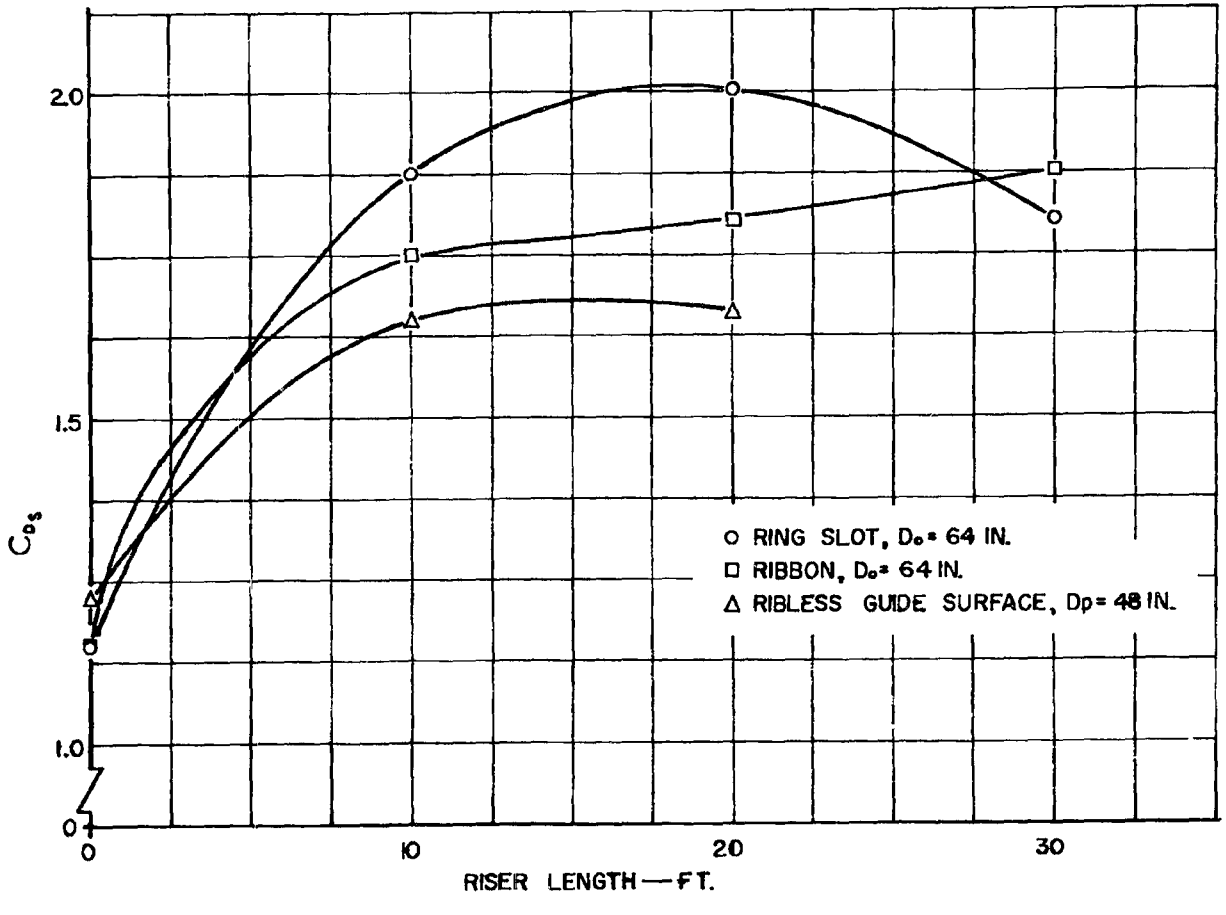

FIG. 38- SYSTEM DRAG COEFFICIENT VERSUS RISER LENGTH FOR DIFFERENT PARACHUTE - CONTAINER COMBINATIONS $Re = 5.49 \times 10^5$; $q = 5.20$ LB/FT^2

that for the same riser length, the system drag coefficient is larger for the ring slot parachute container configuration than either the ribbon or ribless guide surface configurations for all riser lengths except 0 (no riser) where all the three configurations have substantially the same system drag coefficient.

The 64 in. ribbon and the 48 in. ribless guide surface configurations have appreciably the same system drag coefficients for all riser lengths tested.

Figure 39 presents the average system drag coefficient for all types of container-parachute configurations with risers up to 30 ft full scale. The average component drag coefficients and the summation of the component drag coefficients are also given in every case.

Figure 40 graphically illustrates the average system drag coefficients of various container-parachute combinations with the different riser lengths affording a ready means of comparing the different configurations and the effect of riser length for the same configuration.

3.6.3 Parachute and Container Free Attitude Angles

After recording the moment and drag characteristics of the different configurations with risers, the locking arrangement on the pivotal shaft was released, the container angular measuring device and the parachute attitude measuring device were activated and the free attitude angles α , θ , and ψ for different sizes of the ring slot, ribbon, and ribless guide surface parachutes in conjunction with the A-22 Container models with risers representing 10, 20, and 30 ft full scale

CONFIGURATION AND FULL SCALE PARACHUTE DIAMETER (IN.)	RISER LENGTH (FT.)	DRAG COEFFICIENT BASED ON CONTAINER BASE AREA			
		C_{D_P} (PARACHUTE)	C_{D_C} (CONTAINER)	$C_{D_P}+C_{D_C}$ (PARACHUTE + CONTAINER)	C_{D_S} (SYSTEM)
RING SLOT D_o = 96 IN.	0	2.19	0.95	3.14	2.66
	10	2.10	0.95	3.05	3.11
	20	2.14	0.95	3.09	3.01
	30	2.06	0.95	3.01	2.88
RIBBON D_o = 96 IN.	0	1.99	0.95	2.94	2.38
	10	1.98	0.95	2.93	2.65
	20	1.96	0.95	2.91	2.59
	30	1.94	0.95	2.89	2.81
RIBLESS GUIDE SURFACE D_p = 72 IN.	0	1.90	0.95	2.85	2.55
	10	1.85	0.95	2.80	2.66
	20	1.83	0.95	2.78	2.48
	30	1.73	0.95	2.68	2.31
RING SLOT D_o = 64 IN.	0	0.97	0.80	1.77	1.17
	10	0.94	0.80	1.74	1.89
	20	0.88	0.80	1.68	2.05
	30	0.85	0.80	1.65	1.80
RIBBON D_o = 64 IN.	0	0.89	0.80	1.69	1.16
	10	0.88	0.80	1.68	1.77
	20	0.85	0.80	1.65	1.80
	30	0.88	0.80	1.68	1.87
RIBLESS GUIDE SURFACE D_p = 48 IN.	0	0.85	0.80	1.65	1.23
	10	0.80	0.80	1.60	1.65
	20	0.80	0.80	1.60	1.65
	30	0.80	0.80	1.60	NO DATA

FIG. 39- AVERAGE DRAG COEFFICIENTS FOR A-22 CONTAINER AND VARIOUS PARACHUTE SIZES AND TYPES WITH VARIOUS RISER LENGTHS.

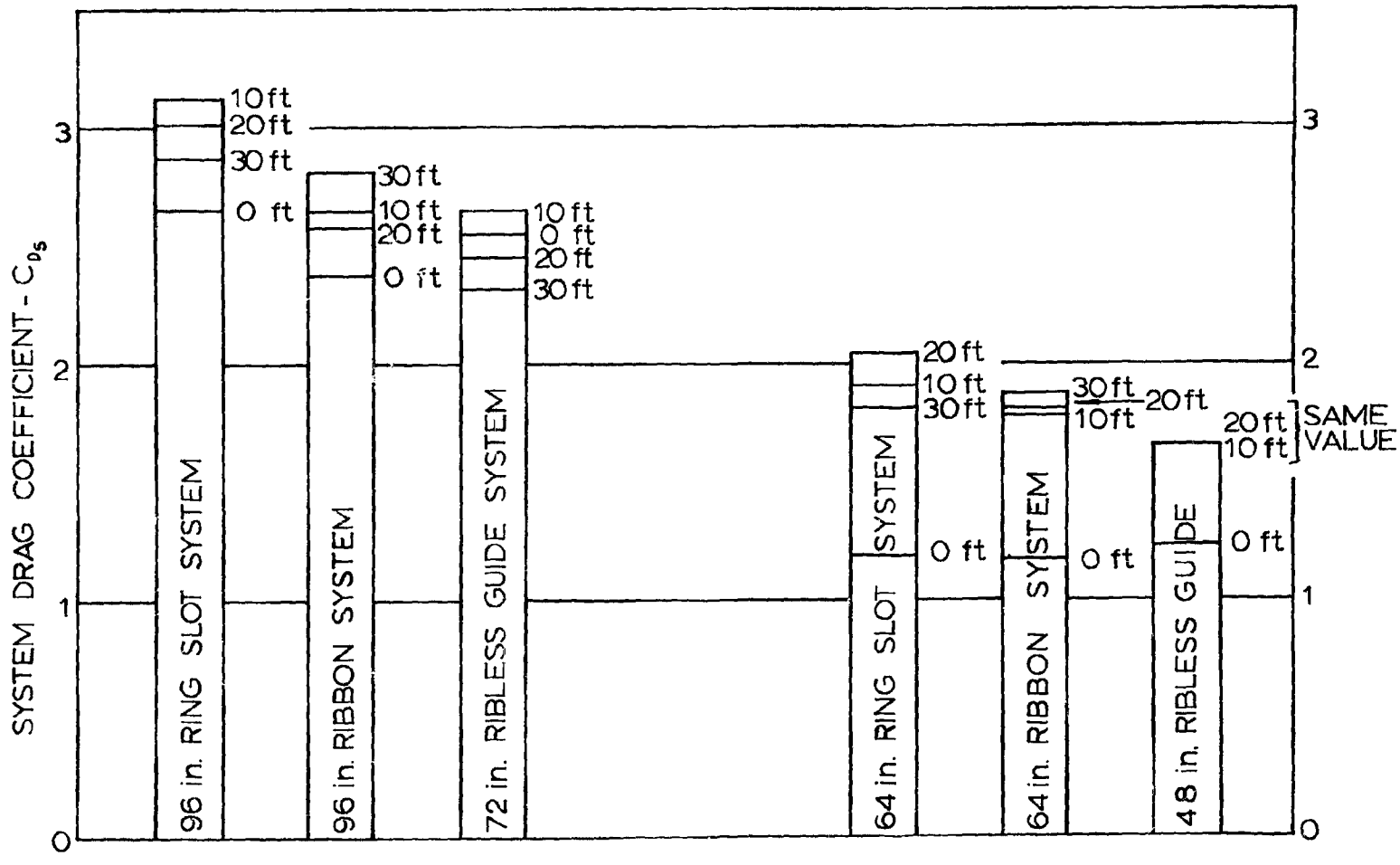

FIG. 40 - DRAG COEFFICIENTS FOR VARIOUS CONTAINER - PARACHUTE COMBINATIONS WITH VARIOUS RISER LENGTHS

REFFERENCE AREA 15.53 SQ. FT. FULL SCALE

were recorded. Figure 41-A, B, and C are photographs of the experimental arrangement representing the A-22 Container in combination with the 64 in. ring slot and ribbon parachutes and the 48 in. ribless guide surface parachute with risers representing 10 ft full scale.

Typical galvanometer traces representing the instantaneous free attitude angles α and θ for the three types of parachutes with risers representing 10 ft full scale are given in Figs 42-A, B, and C.

Using the galvanometer traces for the deflection angles α and θ, mean values of these angles were calculated for each configuration and riser length. As indicated in Paragraph 3.5.3, the weight of the parachute model tends to produce an angle ψ which, because of the horizontal disposition of the riser and parachute axis, is not representative of actual aerial delivery conditions where the path is essentially vertical for most of the trajectory after full deployment. Therefore the angle ψ will not be considered.

The mean values of the angles θ versus α for the different riser lengths are illustrated in Figs 43-A, B, and C for the ring slot, ribbon and ribless guide surface configurations respectively.

We do not suggest that the free attitude angles, as recorded by the galvanometer, represent quantitatively the full scale free flight case. Furthermore, the equilibrium angles appear to depend to a certain extent on the initial rigging alignment. However, the tests give a useful indication

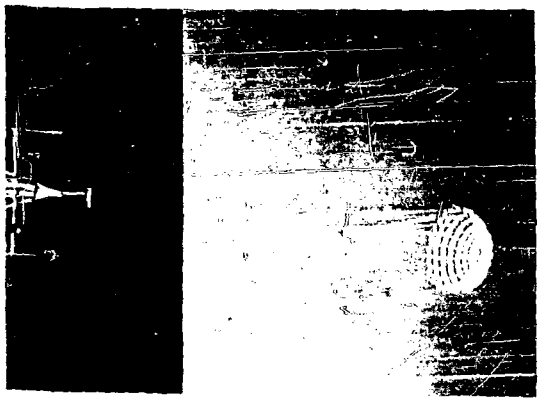

A. MODEL ARRANGEMENT REPRESENTING CONTAINER AND 20% POROSITY 64" DIA. RING SLOT PARACHUTE

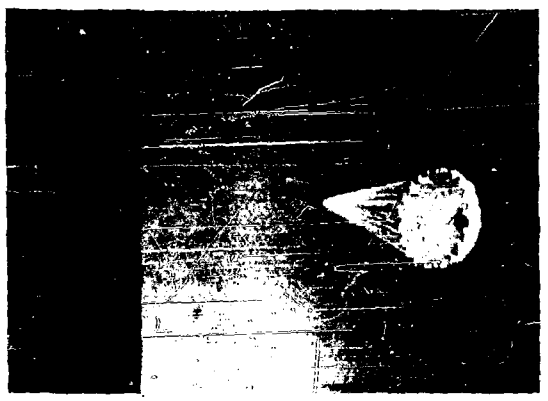

B. MODEL ARRANGEMENT REPRESENTING CONTAINER AND 20% POROSITY 64" DIA. RIBBON PARACHUTE

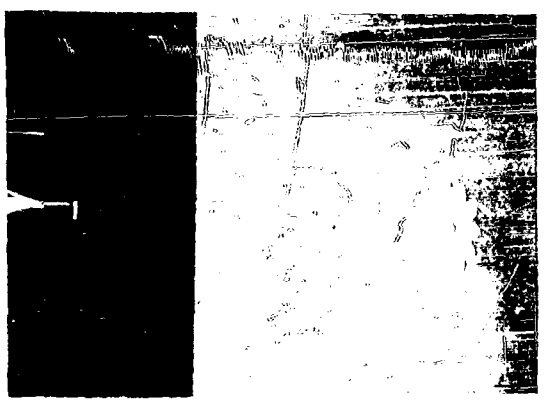

C. MODEL ARRANGEMENT REPRESENTING CONTAINER AND 48" DIA. RIBLESS GUIDE SURFACE PARACHUTE

FIG. 41- EXPERIMENTAL ARRANGEMENT OF THE 1/4 SCALE A-22 CONTAINER IN COMBINATION WITH THREE PARACHUTE TYPES WITH 10 FT RISERS

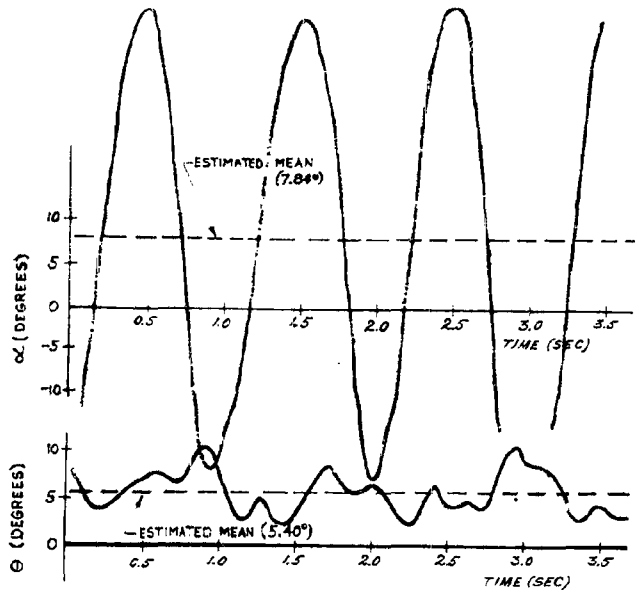

A.- 1/4 Scale Model of Container with 64" Dia. Ring Slot Parachute

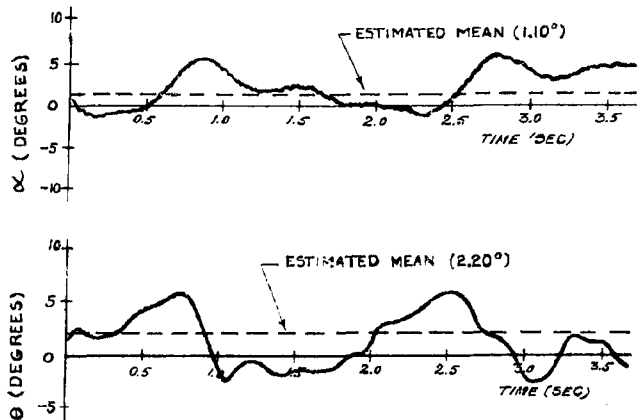

B.- 1/4 Scale Model of Container with 64" Dia. Ribbon Parachute

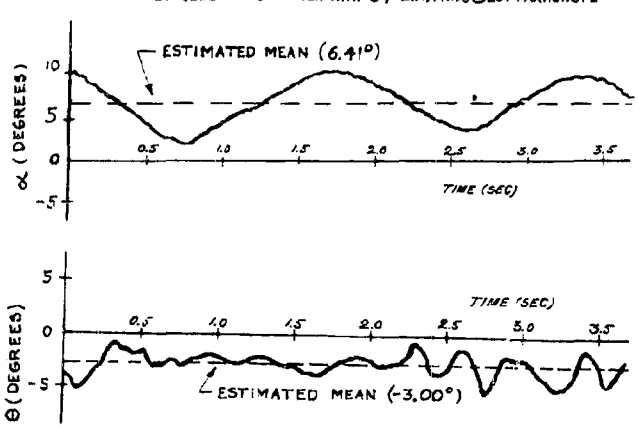

C.- 1/4 Scale Model of Container with 48" Dia. Ribless Guide Surface Parachute

FIG. 42 - COMPARATIVE STABILITY BEHAVIOR OF THE A-22 CONTAINER WITH VARIOUS TYPES OF PARACHUTES AND 10 FT. RISERS.

CONTAINER AND PARACHUTE ATTITUDE ANGLES α AND θ VERSUS TIME.

$Re = 5.49 \times 10^5$.

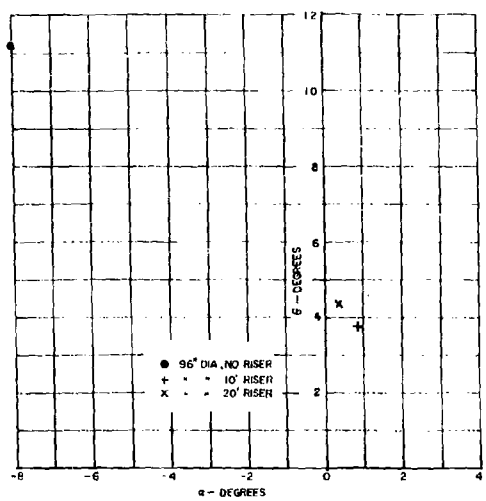

A - 1/6 SCALE MODEL REPRESENTING CONTAINER WITH 96" DIA. SOLID FLAT PARACHUTE

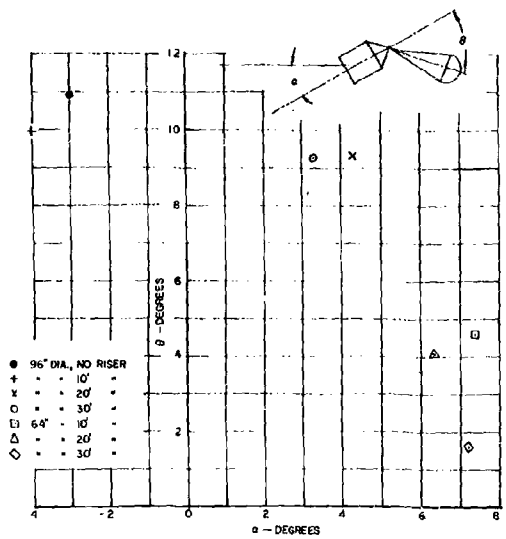

B. - 1/6 AND 1/4 SCALE MODELS REPRESENTING CONTAINER WITH 96" AND 64" DIA RING SLOT PARACHUTE

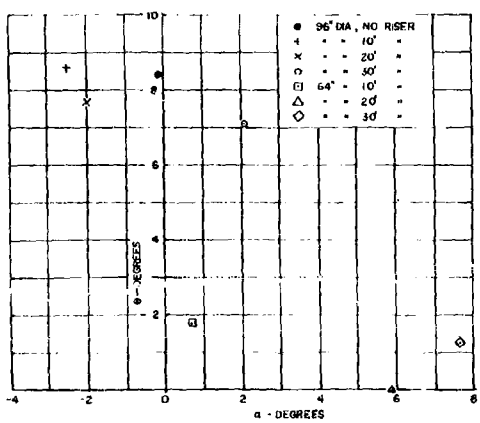

C - 1/6 AND 1/4 SCALE MODELS REPRESENTING CONTAINER WITH 96" AND 64" DIA RIBBON PARACHUTE

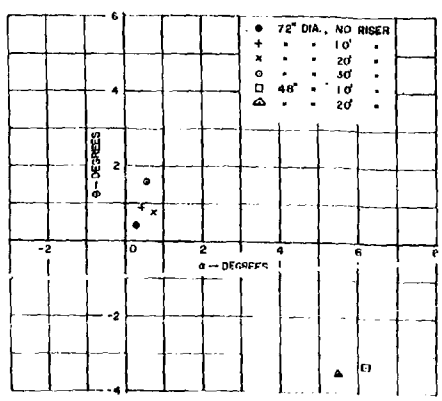

D - 1/6 AND 1/4 SCALE MODELS REPRESENTING CONTAINER WITH 72" AND 48" DIA RIBLESS GUIDE SURFACE PARACHUTE

FIG 43- MEAN ATTITUDE ANGLES α VERSUS θ FOR MODELS OF A-22 CONTAINER AND VARIOUS PARACHUTES WITH DIFFERENT RISER LENGTHS

of the general behavior and relative merits of the different configurations.

IV. CONCLUSIONS AND GENERAL REMARKS

4.1 Conclusions

The experimental results presented in Section III, cover a wide range of configurations involving three different scale models of the A-22 Container, each stabilized by four different types of parachutes using risers representing 0, 10, 20, and 30 ft in full scale.

In addition to the moment characteristics at different angles of attack of the container's longitudinal axis relative to the air flow, the drag at zero angle of attack and the equilibrium angle of attack of the container (α) and the attitude angles (θ and ψ) of the parachute axis with respect to the container's longitudinal axis were recorded thereby providing additional information on the relative merits of the different parachute types as stabilizers and retarders for the A-22 Container. From the results of these experiments, the following general conclusions may be made:

a) The maximum height configuration of the A-22 Container (60 in. full scale) has the more critical stabilization requirements, i.e., it has the smaller stable range and stable moment coefficients in that range and the larger destabilizing moments outside that range.

b) Without risers, the A-22 Container may be stabilized by means of parachutes having a nominal diameter,

D_o = 96 in. for the solid flat, ring slot (20% porosity) or ribbon types (20% porosity) and having a projected diameter D_p = 72 in. for the ribless guide surface type.

c) With a minimum riser length of 10 ft, the A-22 Container may be stabilized over the full angular range by means of parachutes having a nominal diameter D_o = 64 in. for the solid flat, ring slot, or ribbon types and a projected diameter D_p = 48 in. for the ribless guide surface type.

d) The use of risers greatly helps in stabilizing the container, particularly for the relatively large scales and more especially at large angle of attack. There appears, however, to be an optimum length of riser beyond which the moment coefficient does not increase with increase of riser length and in some cases even tends to decrease.

e) The system drag coefficient is greatly increased by using a riser and, in most cases, with a minimum riser of 10 ft full scale, it becomes substantially equal to the sum of the drag coefficients of the container and parachute models taken separately when both are referred to the container base area.

f) From a visual observation of model behavior in the wind tunnel and a study of the free attitude angles of the container and parachute, we find that the configurations involving the solid flat parachute, with or without risers, exhibit large amplitude random motion and violent oscillations. It is concluded that this type of parachute, despite its larger drag and restoring moment coefficients, is the least suitable for the proposed application.

The configurations involving the ring slot parachute exhibited, in general, medium amplitude container deflections and parachute oscillations and were decidedly more suitable than those with the solid flat type.

The various configurations using the ribbon and ribless guide surface parachute types produced, in general, much smaller amplitude container deflections and parachute oscillations and appeared to be quite satisfactory. The frequency of oscillation of the parachute was higher for the ribless guide surface, but the amplitudes were generally much smaller, and this type appeared to be the most suitable one from the container and parachute deflection point of view.

4.2 Additional Remarks

The aerodynamic parameters presented in the preceding chapters appear to be satisfactory for trajectory calculations from which the performance characteristics and operational requirements of the various combinations could be estimated.

REFERENCES

1. Department of the Army Technical Manual, TM 10-530, June, 1952.

2. United States Air Force Parachute Handbook, WADC TR 55-265, December, 1956.

3. White, Gerald B.: Principles of High Velocity Dropping of Aerial Cargo, Parachute Engineering and Retardation Summer Course, July 14-25, 1958, University of Minnesota.